Int J Clin Exp Med (2008) 1, 213-247
www.ijcem.com/IJCEM805005

Original Article

Prevention of Trauma and Hemorrhagic Shock-Mediated Liver Apoptosis by Activation of Stat3α

Ana Moran[1], Ayse Akcan Arikan[2], Mary-Ann A. Mastrangelo[1], Yong Wu[1], Bi Yu[1], Valeria Poli[3] and David J. Tweardy[1,4]

[1]Infectious Diseases Section and Department of Medicine, Baylor College of Medicine, Houston, TX,USA; [2]Critical Care Section and Department of Pediatrics, Baylor College of Medicine, Houston, TX, USA; [3]Department of Genetics, Biology and Biochemistry, University of Turin, Turin, Italy; [4]Department of Molecular and Cellular Biology, Baylor College of Medicine, Houston,TX, USA

Received May 14, 2008; accepted June 6, 2008; available online June 15, 2008

Abstract: Trauma is a major cause of mortality in the United States. Death among those surviving the initial insult is caused by multiple organ failure (MOF) with the liver among the organs most frequently affected. We previously demonstrated in rodents that trauma complicated by hemorrhagic shock (trauma/HS) results in liver injury that can be prevented by IL-6 administration at the start of resuscitation; however, the contribution of the severity of HS to the extent of liver injury, whether or not resuscitation is required and the mechanism for the IL-6 protective effect have not been reported. In the experiments reported here, we demonstrated that the extent of liver apoptosis induced by trauma/HS depends on the duration of hypotension and requires resuscitation. We established that IL-6 administration at the start of resuscitation is capable of completely reversing liver apoptosis and is associated with increased Stat3 activation. Microarray analysis of the livers showed that the main effect of IL-6 was to normalize the trauma/HS-induced apoptosis transcriptome. Pharmacological inhibition of Stat3 activity within the liver blocked the ability of IL-6 to prevent liver apoptosis and to normalize the trauma/HS-induced liver apoptosis transcriptome. Genetic deletion of a Stat3β, a naturally occurring, dominant-negative isoform of the Stat3, attenuated trauma/HS-induced liver apoptosis, confirming a role for Stat3, especially Stat3α, in preventing trauma/HS-mediated liver apoptosis. Thus, trauma/HS-induced liver apoptosis depends on the duration of hypotension and requires resuscitation. IL-6 administration at the start of resuscitation reverses HS-induced liver apoptosis, through activation of Stat3α, which normalizes the trauma/HS-induced liver apoptosis transcriptome.

Key Words: Nucleosomes, TUNEL, expression Microarray, transcriptome

Introduction

Trauma is the leading cause of death for those under 45 years old in the United States [1]. While almost half of the deaths occur at the time of the injury, the leading cause of death among those surviving the initial insult is multiple organ failure (MOF) [2, 3]. The liver is one of the organs most frequently affected by trauma and hemorrhagic shock, and its central role in metabolism and homeostasis makes this organ a critical one for survival of the host after severe injury [4, 5].

We previously demonstrated in rats and mice that trauma complicated by hemorrhagic shock (trauma/HS) results in liver injury as evidence by hepatocyte apoptosis [6], liver necrosis [7] and elevated transaminases [8]; however, the contribution of the severity of hemorrhagic shock to the extent of liver injury and whether or not resuscitation is required for liver injury to occur have not been reported. We also previously demonstrated that administration of IL-6 at the start of resuscitation prevented liver apoptosis and necrosis [6, 7]. IL-6 activates two anti-apoptotic signaling pathways, one involving Akt and the other involving signal transducer and activator or transcription (STAT)3. Whether or not one or both pathways are involved in the

anti-apoptotic effect of IL-6 has not been determined.

In the experiments reported here, we investigated the hypotheses: 1) that trauma/HS-induced liver apoptosis depends on the severity of hemorrhagic shock and requires resuscitation; and 2) that the protective effect of IL-6 administration is mediated by Stat3. We demonstrated that the extent of liver apoptosis induced by our model of trauma/HS depends on the duration of hypotension and requires resuscitation. We established that IL-6 administration at the start of resuscitation following the longest duration of hypotension is capable of completely reversing liver apoptosis and is associated with increased Stat3 activation. Microarray analysis of the livers showed that the main effect of IL-6 was to normalize the trauma/HS-induced apoptosis transcriptome. Pharmacological inhibition of Stat3 activity within the liver blocked the ability of IL-6 to prevent liver apoptosis and to normalize the trauma/HS-induced liver apoptosis transcriptome. Genetic deletion of a Stat3β, a naturally occurring, dominant-negative isoform of the Stat3, attenuated trauma/HS-induced liver apoptosis, confirming a role for Stat3, especially Stat3α, in preventing trauma/HS-mediated liver apoptosis. Thus, trauma/HS-induced liver apoptosis depends on the duration of hypotension and requires resuscitation. IL-6 administration at the start of resuscitation reverses HS-induced liver apoptosis, through activation of Stat3α, which normalizes the trauma/HS-induced liver apoptosis transcriptome.

Materials and Methods

Rat and mouse protocols for trauma plus hemorrhagic shock

These studies were approved by the Baylor College of Medicine Institutional Review Board for animal experimentation and conform to National Institutes of Health guidelines for the care and use of laboratory animals. Adult male Sprague-Dawley rats were obtained from Harlan (Indianapolis, IN). Stat3β homozygous-deficient ($Stat3\beta^{\Delta/\Delta}$) mice were generated as described [9] and re-derived at Jackson labs. Pups from heterozygous matings were tailed and genotyped by PCR, as described, with minor modifications [9].

Eight-week old male Sprague-Dawley rats (200-250 gm) were used for all experiments in this study. Rats were subjected to the sham or hemorrhagic shock (HS) protocols, as described [10, 11] with modifications. Blood was withdrawn into a heparinized syringe episodically to maintain the target MAP at 35 mmHg until blood pressure compensation failed. Blood was then returned as needed to maintain the target MAP. The amount of shed blood returned (SBR) defined 5 different levels of shock severity reflected in the duration of hypotension: 0% SBR (SBR0) represented the lowest level of shock severity (duration of hypotension, 78 ± 2.5 minutes), 10% SBR (SBR10; duration of hypotension, 149 ± 41.4 minutes), 20% SBR (SBR20; duration of hypotension, 165 ± 32.7 minutes), 35% SBR (SBR35; duration of hypotension, 211 ± 7.6 minutes), and 50% SBR (SBR50; duration of hypotension, 273 ± 24.9 minutes). At the end of the hypotensive period, rats were resuscitated as described [10, 11] and humanely sacrificed 60 minutes after the start of resuscitation. Where indicated, rats received 10 μg/kg of recombinant human IL-6 in 0.1 ml PBS at the initiation of the resuscitation or PBS alone. Sham rats were anesthetized and cannulated for 250 minutes but were not subjected to hemorrhage or resuscitation. One group of rats (UHS) was subjected to the most severe hemorrhagic shock protocol (50% SBR), but not resuscitated and kept at the target MAP (35 mmHg) for an additional 60 minutes (duration of hypotension = 336 ± 10.3 minutes) before sacrifice.

$Stat3\beta^{\Delta/\Delta}$ mice and wild-type littermate mice were subjected to a trauma/HS protocol [8,12], which was similar to the rat protocol except that the target MAP in the mouse was 30mm Hg and the duration of hypotension was 180 min in all mice. Sham mice were anesthetized and immobilized in a pair-wise fashion with HS mice and sacrificed at the same time as their HS companion.

Rat and mouse livers were harvested immediately after sacrifice. The right liver lobe was fixed with paraformaldehyde solution (2%) for histologic analysis and the left lobe was snap frozen in liquid nitrogen for protein and RNA extraction.

In vivo pharmacological inhibition of Stat3

To achieve pharmacological inhibition of Stat3 activity within the lungs of rats, rats were randomized to receive by tail vein injection the G-rich, quartet-forming oligodeoxynucleotide (GQ-ODN) T40214 or nonspecific (NS)-ODN (2.5 mg ODN/kg) complexed in polyethyleneimine, as described [13], 24 hours prior to subjecting them to the SBR50 protocol with IL-6 treatment. The half-life of T40214 in tissues is ≥ 48 hr [14].

Nucleosome ELISA

Levels of histone-associated DNA fragments (nucleosomes) were determined in liver homogenates with an ELISA method (Cell Death Detection ELISAplus; Roche Diagnostics, Manheim, Germany). Frozen livers were cut by cryotome into 5 micron sections and resuspended in cell lysis buffer using the reagents from the ELISA kit. The lysates were sonicated in ice 3 times, 10 seconds each, centrifuged and supernatants harvested. Total protein concentration of each supernatant was determined by Bradford assay (Bio-Rad Protein Assay, Bio-Rad Laboratories, Inc., Hercules, CA). Equal amounts of protein (200ug) were loaded into microtiter wells in duplicate. A positive control (lyophilized, stabilized nucleosome concentrate of known concentration, provided in the kit) and a negative control (water) were also loaded in duplicate. Serial dilutions of the positive control were loaded in duplicate and used to plot a standard curve. The nucleosome concentration for each sample was obtained by plotting each sample duplicate's OD against the standard curve. The final sample nucleosome concentration was the average of the duplicates [15]. The rest of the assay was performed according to manufacterer's instructions.

Terminal deoxynucleotidyl transferase (TdT) mediated nick end labeling (TUNEL) staining

TUNEL staining to enzymatically detect the free 3'-OH termini was performed using the ApopTag Plus Peroxidase in situ Apoptosis Detection Kit from Chemicon International. Slides were rehydrated from Xylene to PBS through a series of decreasing concentrations of ethanol and digested in proteinase K (20 ug/ml) for 3 minutes at 23°C. Endogenous peroxidases were quenched for 30 minutes in 3% hydrogen peroxide in PBS. TdT enzyme was diluted in TUNEL solution buffer then used as suggested by the manufacturer. Slides were counterstained with hematoxyllin. TUNEL positive cells were assessed microscopically by counting the total nuclei and the number of TUNEL-positive nuclei in twenty random 1000x fields by an experienced histologist, blinded to the treatment each rat received. Data is presented as the number of TUNEL positive cells per high power field (hpf).

Immunoblotting

Levels of STAT3 activation within the livers of rats were assessed by immunoblotting using whole-tissue extracts of liver sections with mouse monoclonal antibody to Tyr705 phosphorylated (p)STAT3 (Cell Signaling Technology, Inc., Danvers, MA; 1:1000 dilution). Briefly, frozen livers were cut by cryotome into 5 micron sections and resuspended in cell lysis buffer (Cell Death Detection ELISAplus Kit, Roche Diagnostics, Manheim, Germany). The supernatant was sonicated in ice 3 times, 10 seconds each. Samples were then centrifuged and the supernatant evaluated by Bradford assay for total protein quantification. Protein samples (60ug total protein) were separated by SDS-PAGE and transferred to a PVDF membrane. The membrane was incubated overnight with mouse monoclonal antibody and subsequently incubated with goat antimouse antibody with horseradish peroxidase (HRP) conjugate (Zymed, San Francisco, CA) for 1 hour. ECL agent (Amersham Biosciences, UK) was used for detection. The membrane was then stripped (using RestoreTM Western Blot Stripping Buffer, PIERCE, Rockford, IL) and immuoblotting performed to detect total STAT3 protein in the whole tissue extracts of livers using mouse IgG1 monoclonal antibody to STAT3 (BD Biosciences, Rockville, MD). Densitometry was performed using ImageQuant TL v2005 software (Amersham Biosciences, Buckinghamshire, England). Results are expressed as the ratio of pSTAT3 signal (after background signal subtraction) to total STAT3 signal (after background signal subtraction) for each sample.

RNA isolation and microarray hybridization and analysis procedures

Total RNA was isolated from 4-5 micron cryotome sections of liver using TRIzol® Reagent (Invitrogen, Carlsbad, California) single step RNA isolation protocol followed by

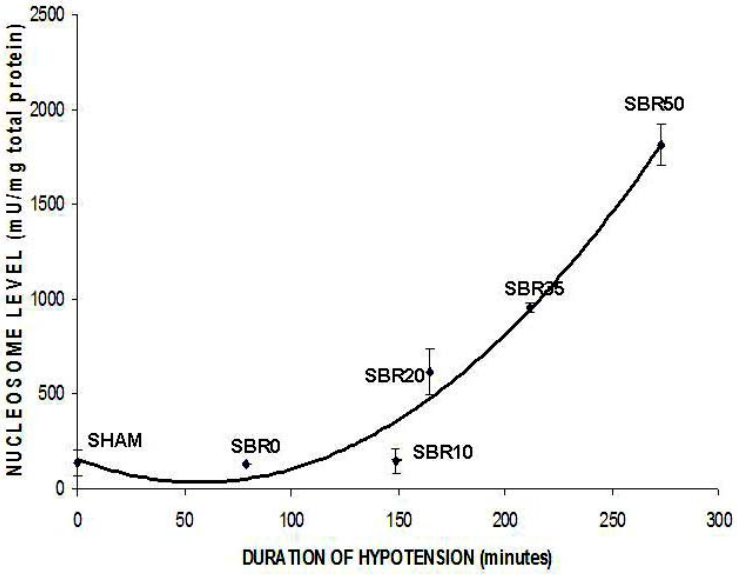

Figure 1. Effect of shock severity on liver apoptosis. Rats were subjected to sham protocol (S) or to trauma/HS protocol with increasing duration of shock as indicated followed by resuscitation. The livers were harvested 60 minutes after the start of resuscitation. Nucleosome levels were measured in protein extracts of frozen sections of each liver and the results plotted after correction for total protein, as a function of the duration of the hypotensive period for each animal. Curve fitting was performed and the best-fitting curve shown; nucleosome levels increased exponentially with duration of hypotension (Pearson correlation coefficient=0.879, p<0.001).

purification with RNeasy® Mini Kit (QIAGEN, Hilden, Germany) as instructed by the RAE 230A following Affymetrix protocols used within the Baylor College of Medicine Microarray Core Facility. Gene expression profiling was performed with the Affymetrix Rat Array.

Microarray Analysis

We used Affymetrics GCOS, dChip and Array Analyzer (Insightful Corporation) software packages for quality assessment and statistical analysis and annotation. Expression estimation and group comparisons were done with Array Analyzer. Low-level analyses included background correction, quartile normalization and expression estimation using GCRMA [16]. One-way analysis of variance (ANOVA) with contrasts [17] was used for group comparisons on all genes and on the list of apoptosis related genes only. P-values were adjusted for multiple comparisons using the Benjamini-Hockberg method [18]. The adjusted p-values represent false discovery rates (FDR) and are estimates of the proportion of "significant" genes that are false or spurious "discoveries". We used a FDR=10% as cut-off.

Statistical Analysis

Data are presented as mean ± standard error of the mean (SEM). Multiple group comparisons of means were done by one-way analysis of variance (ANOVA). Post hoc analysis was done by Student-Newman-Keuls test for 2-group comparisons of means. Correlation between duration of hypotension and nucleosome levels was done for each individual study animal by Pearson correlation coefficient. Goodness of fit was evaluated by R-square. All statistical analyses were done on SigmaStat 3.5 (SYSTAT Software Inc., Chicago, IL).

Results

HS-induced liver apoptosis depends on the severity of shock

To confirm our previous findings that trauma/HS induces liver apoptosis, to determine if apoptosis is an early event following trauma/HS as well as to evaluate the contribution of the severity of shock in our rat model of trauma/HS, we measured histone-associated DNA fragments (nucleosomes) in the livers of rats subjected to increasing severity of shock 1 hr after the initiation of resuscitation. Nucleosome levels increased exponentially with increasing duration of shock (Pearson correlation coefficient 0.879, p<0.001) with the level of nucleosomes in the SBR50 group (1817.3 ± 105.9 units/ml) achieving a level 13.1 times higher than sham (139 ± 67 units/ml; p<0.001, ANOVA; **Figure 1**). Thus, trauma/HS-induced liver apoptosis occurs within 1 hr of resuscitation and depends on the severity of shock.

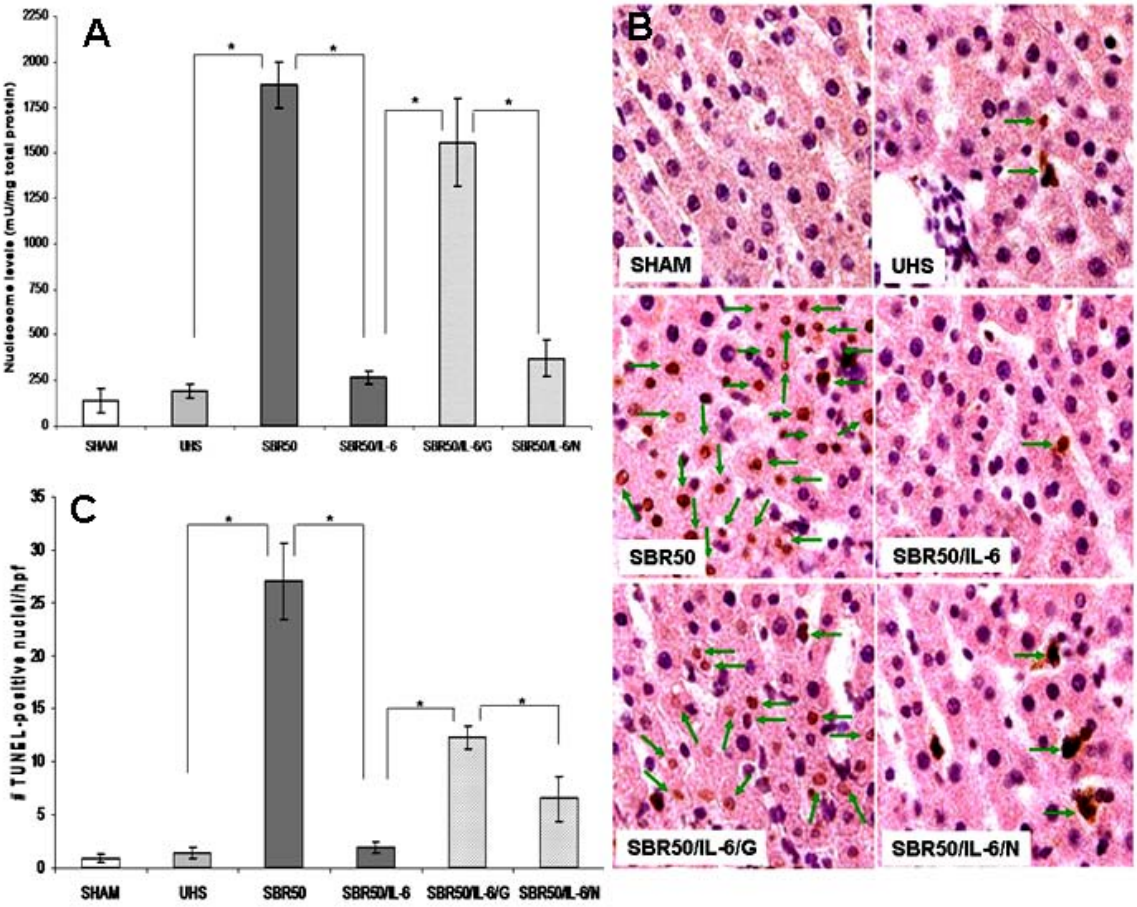

Figure 2. Effect of resuscitation, IL-6 treatment and GQ-ODN pre-treatment on HSinduced liver apoptosis. Rats were subjected to sham protocol (Sham, n=3), unresuscitated hemorrhagic shock (UHS, n=3), HS treated with placebo at the beginning of resuscitation (SBR50, n=4), HS treated with IL-6 at the beginning of resuscitation (SBR50/IL-6, n=4), HS preceded by treatment with GQ oligodeoxynucleotide (GQ-ODN) 24 hours prior to resuscitation with IL-6 (SBR50/IL-6/G, n=3), or HS preceded by treatment with nonspecific-ODN (NS-ODN) 24 hours prior to resuscitation with IL-6 (SBR50/I-6/N, n=3). The livers were harvested 60 minutes after the start of resuscitation. Nucleosome levels were measured in protein extracts of frozen sections of each liver (Panel A). Data presented are mean + SEM of nucleosome level corrected for total protein for each group. Bars marked with an asterisk (*) differ significantly within the pair ($p<0.05$). In panel B, sections of paraformaldehyde-fixed liver were stained using the TUNEL assay. Representative photomicrographs of 1000x fields of liver specimens from each experimental group are shown. Apoptotic nuclei are indicated by arrows. In panel C, TUNEL-positive nuclei were counted; data shown are the mean ± SEM number of TUNELpositive nuclei per 1000x fields (20 fields counted). Bars marked with an asterisk (*) differ significantly within the pair ($p<0.05$).

Trauma/HS-induced liver apoptosis requires resuscitation

To determine the specific contribution of resuscitation to liver apoptosis, we assessed nucleosome levels as well as number of TUNEL-positive cells in the livers of rats subjected to HS without resuscitation (UHS group) and compared these results with those obtained in the sham and the resuscitated SBR50 groups. The level of nucleosomes in the UHS group (193 ± 36 units/mg total protein) was statistically indistinguishable from that of the sham group (139 ± 67 units/mg total protein; **Figure 2A**). Similar results were obtained when liver apoptosis was assessed by TUNEL staining. The number of TUNEL-positive nuclei/hpf in the UHS group (1.4 ± 0.5; **Figure 2B, C**) similar to that of the sham group (0.9 ± 0.4). In addition, histological evaluation of the cells containing TUNEL-

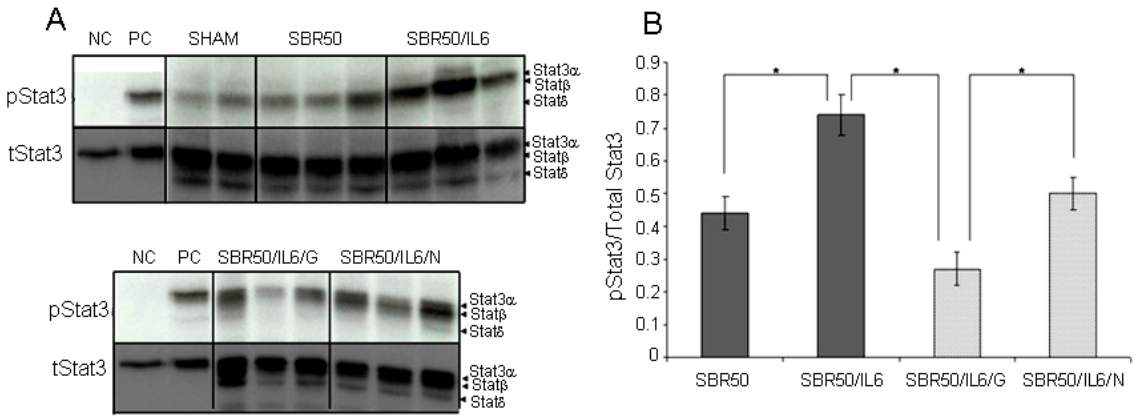

Figure 3. Effect of IL-6 treatment and GQ-ODN pre-treatment on Stat3 activity within the livers. Rats were subjected to the sham protocol or HS protocol and treated with placebo at the beginning of resuscitation (SBR50), HS treated with IL-6 at the beginning of resuscitation (SBR50/IL-6), HS preceded by treatment with GQ-oligodeoxynucleotide (GQ-ODN) 24 hours prior to resuscitation with IL-6 (SBR50/IL-6/G), or HS preceded by treatment with nonspecific-ODN (NS-ODN) 24 hours prior to resuscitation with IL-6 (SBR50/IL-6/N). The livers were harvested 60 minutes after the start of resuscitation. In panel A, protein extracts of whole liver were separated by SDS-PAGE and immunoblotted for phosphorylated (p)Stat3 and total Stat3 (NC = negative control, HepG2 cells incubated with PBS for 30 minutes prior to protein extraction; PC = positive control, HepG2 cells incubated with IL-6, 30 ng/ml for 30 minutes prior to protein extraction). In panel B, the pStat3 and total Sta3 bands were quantitated by densitometry and data presented as mean ± SEM of pStat3 signal corrected for total Stat3 signal for each group. Bands representing Stat3α, Stat3β and Stat3δ are indicated on the right [54, 55]. Bars marked with an asterisk (*) differ significantly within the pair ($p<0.0001$).

positive nuclei revealed that more than 80% were hepatocytes, a key parenchyma cell.
Thus, apoptosis within the liver following trauma/HS requires resuscitation. The fact that no liver apoptosis occurs without resuscitation suggests that complete prevention of liver apoptosis may occur with an appropriate intervention introduced at the start of resuscitation.

IL-6 administration at the beginning of resuscitation prevents trauma/HS-induced liver apoptosis through activation of Stat3

In our mouse model of HS, we have previously demonstrated that IL-6 administration at the beginning of resuscitation prevented the development of HS-induced liver apoptosis detected 24 hrs after HS [6]. To confirm these findings and to gain an improved molecular and cellular understanding of the anti-apoptotic effects of IL-6, we measured apoptotic cell death in rats subjected to trauma/HS with the most severe HS protocol (50% SBR) and randomly assigned to receive either PBS (SBR50) or IL-6 (10 μg/kg, SBR50/IL-6) at the beginning of resuscitation. Nucleosome levels in the SBR50/IL-6 group (264 ± 36 units/ml) were decreased 3.3 times compared to those of the SBR50 group (874 ± 127 units/ml, $p<0.001$) and were similar to sham levels (139 ± 67 units/ml; **Figure 2A**). TUNEL staining confirmed these results. The number of TUNEL-positive nuclei/hpf in the SBR50/IL-6 group (1.9 ± 0.5) was decreased 14.2 times compared to the SBR50 group (27 ± 3.6, $p<0.001$), to levels statistically similar to those of the sham group (0.9 ± 0.4; **Figures 2B and 2C**). Thus, IL-6 administration at the beginning of resuscitation prevents trauma/HS-induced liver apoptosis occurring 1 hr after trauma/HS in rats as well as 24 hrs after trauma/HS in mice [6].

IL-6 binding to IL-Rα and gp130 results in gp130 dimerization and phosphorylation of gp130-associated protein-tyrosine kinases Jak1, Jak2, and Tyk2, which is followed by activation of two major signaling pathways within cells—Stat3 and SHP-2/Grb-2/ERK [19]. The SHP-2/Grb2/ERK pathway bifurcates resulting in activation of p38MAPK and PI-3K. Stat3 and P-I3K/Akt activation, but not p38MAPK, link to anti-apoptotic effects within cells. Stat3 mediates its anti-apoptotic effect in cancer cells through its ability to up-regulate

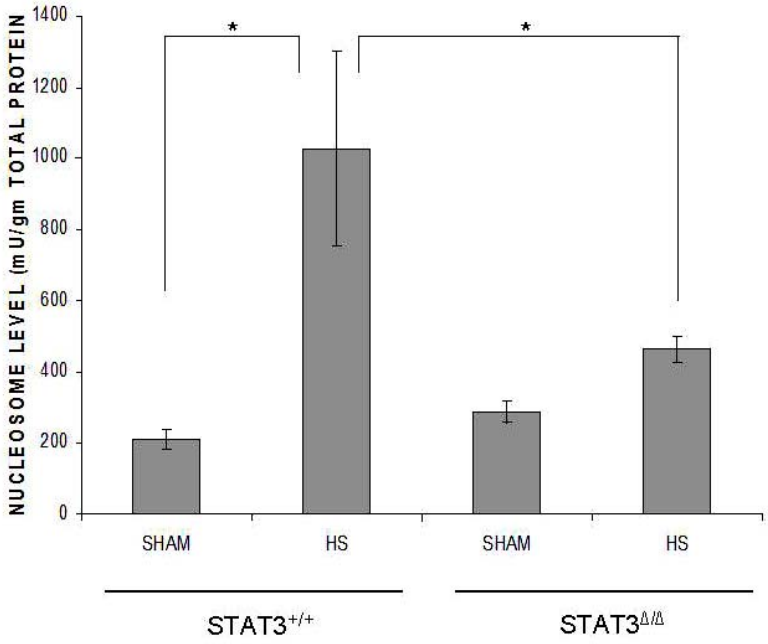

Figure 4. Effect of Stat3β ablation on trauma/HS-induced liver apoptosis. Stat3β homozygous-deficient (Stat3βΔ/Δ) mice and their littermate control wild type mice were subjected to the murine trauma/HS protocol or sham protocol and their livers harvested 1 hr after the start of resuscitation. Nucleosome levels were measured in protein extracts of frozen sections of the liver and the results corrected for total protein. Data presented are the means ± SEM of each group (n ≥ 3). Significant differences are indicated (Student's t-test).

anti-apoptotic genes such as Bcl-xL, Bcl-2 and Mcl-1 [20]. Akt is a highly promiscuous kinase with a large number of binding partners and targets [21] that posttranslationally modify transcription factor systems such as Forkhead [22, 23], IκB/NF-κB and cyclic AMP response element binding protein (CREB) [24], which together result in increased transcription of survival genes and decreased transcription of apoptotic genes [25]. To assess if the anti-apoptotic effects of IL-6 in the liver is mediated by Stat3 activation, we first determined if Stat3 is activated in the livers of rats resuscitated with IL-6. Extracts of cryotome sections of the liver harvested 1 hour after IL-6 treatment were examined by immunoblotting with mouse monoclonal antibody to Tyr705 phosphorylated (p)Stat3 (**Figure 3A**). Densitometric analysis of the signal intensity of the pStat3 bands normalized for total Stat3 indicated that Stat3 activity is increased 1.7 fold in the livers of IL-6-treated rats compared to placebo-treated rats (p=0.002, ANOVA; **Figure 3B**).

To further evaluate the role of Stat3 downstream of IL-6 in mediating its anti-apoptotic effects in the liver, we examined whether or not these effects of IL-6 could be reversed by pretreatment of rats with a G-rich oligodeoxynucleotide, G-quartet (GQ)-ODN, T40214, a novel Stat3 inhibitor, that forms a rigid G-quartet structure within cells and inhibits the growth of tumors in which Stat3 is constitutively activated [13, 14, 26, 27]. Rats were treated in a blinded fashion with GQ-ODN (SBR50/IL-6/G group) or nonspecific (NS) ODN (SBR50/IL-6/N group) 24 hours prior to being subjected to HS and resuscitation with IL-6. Pre-treatment with GQ-ODN reduced Stat3 activity within the livers of HS/I/G rats 1.9-fold compared to HS/I/N rats (**Figures 3A, B**). Importantly, the inhibition of Stat3 activation within the livers of the SBR50/IL-6/G rats was accompanied by a return of nucleosomes (1556 ± 241 units/ml) to levels similar to those of the placebo treated (SBR50) group (1874 ± 127 units/ml, p>0.05) and 11.2 fold higher that those of the IL-6 treated (SBR50/IL-6) group (264 ± 36 units/ml, p<0.001; **Figure 2A**). Similarly, the number of TUNEL-positive nuclei/hpf in livers of rats from the SBR50/IL-6/G group (12.3 ± 1.1) was 6 fold higher than that of the SBR50/IL-6 group (1.9 ± 0.5, p<0.0001); **Figures 2B and C**). Nucleosome levels and number of TUNEL-positive nuclei/hpf in livers of rats pre-treated with NS-ODN were indistinguishable from those of the SBR50/IL-6 group (**Figures 2A and B**). Thus, pharmacological inhibition of Stat3 using GQ-ODN in rats subjected to severe HS resuscitated with IL-6 markedly attenuated IL-6- mediated Stat3 activation and prevention of liver apoptosis.

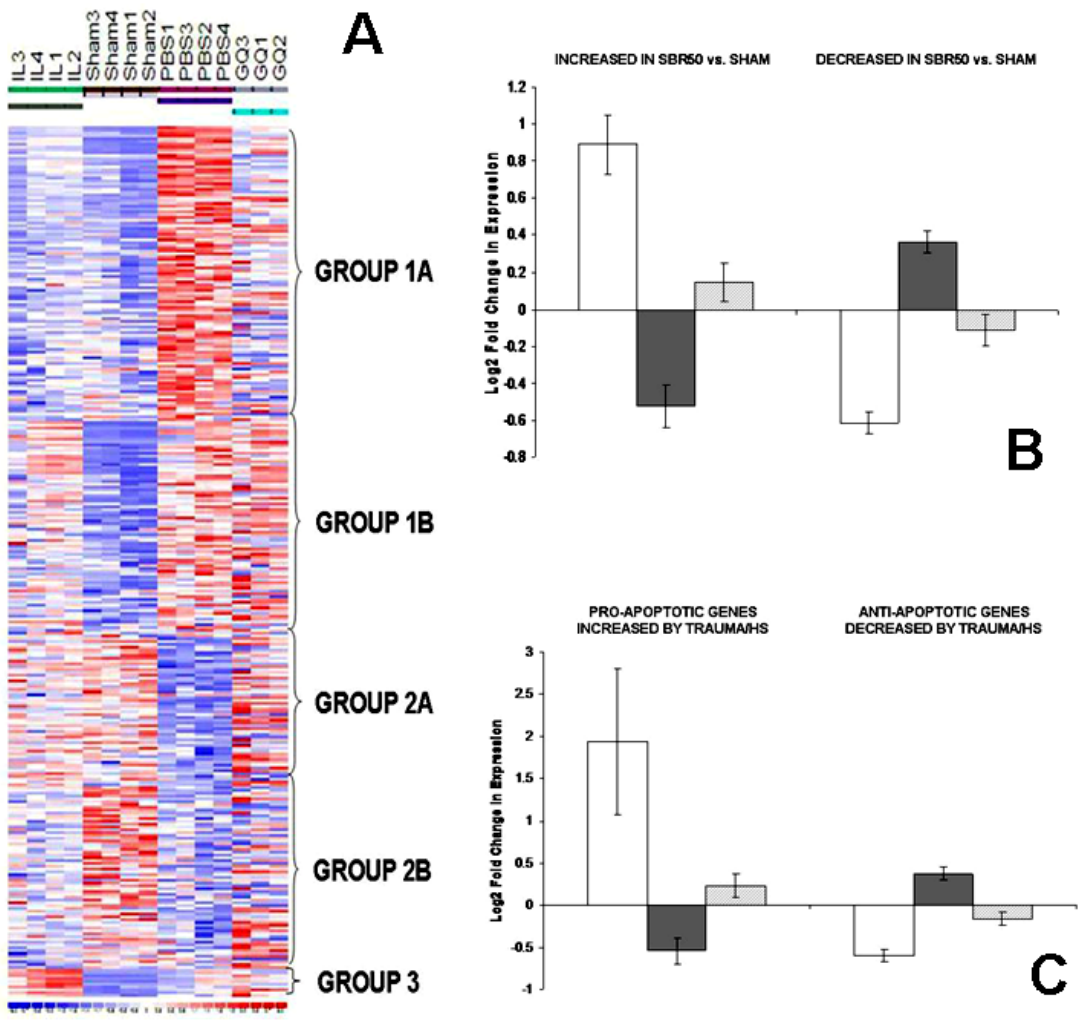

Figure 5. Effect of trauma/HS without or with IL-6 treatment on liver apoptosisrelated gene expression; impact of Stat3 inhibition on the IL-6 effect. In panel A, a heat map of apoptosis pathway genes is shown containing those genes whose expression is altered within the 4 groups. Columns represent samples from the 4 groups examined as indicated (S, Sham; P, placebo-treated SBR50; I, IL-6-treated SBR50/IL-6; and G, animals pre-treated with G-quartet ODN prior to HS and IL-6 treatment, SBR50/IL-6/G). Rows represent genes as listed in Table 1. Red indicates a level of expression above the mean expression of a gene within the experimental group. White indicates a level of expression at the mean within the experimental group while blue indicates a level of expression below the mean within the experimental groups. Log2-fold changes in expression levels of subsets of apoptosis-related genes are shown in panels B and C comparing SBR50 vs. sham (open bars), SBR50/IL-6 vs. SBR50 (gray bars) and SBR50/IL-6/G vs. SBR50/IL-6/N (stippled bars). In panel B, the 308 apoptosis-related genes whose expression levels were changed in SBR50 vs. sham were separated into those genes whose transcript levels were increased in SBR50 vs. sham (134 genes; left side of panel) and those whose transcript levels were decreased in SBR50 vs. sham (90 genes; right side of the panel). Bars shown represent mean ± SD of the Log2-fold change in gene expression levels for each comparison. In panel C, the overall effect of trauma/HS in transcript levels of pro- and antiapoptotic genes is shown. In the left side of the panel, the mean ± SD of the Log2-fold change in gene expression levels of 87 proapoptotic genes whose expression was increased in the SBR50 vs. sham comparison is shown (open bar). The expression of 74 of 87 of these genes was decreased in the SBR50/IL-6 vs. SBR50 comparison (gray bar). In the right side of the panel, the mean ±SD of the Log2-fold change in gene expression levels of 68 anti-apoptotic genes whose expression was decreased in the SBR50 vs. sham comparison is shown (open bar). The expression of 63 of these genes was increased in the SBR50/IL-6 vs. SBR50 comparison (gray bar).

Table 1. Apoptosis-related genes examined in the microarray experiments

#	Accession	Gene Name	Gene Symbol
1	BF417479	24-dehydrocholesterol reductase	Dhcr24
2	NM_022225	5-hydroxytryptamine (serotonin) receptor 1B	Ets1
3	NM_030870	8-oxoguanine DNA-glycosylase 1	Ogg1
4	NM_020306	a disintegrin and metalloproteinase domain 17 (tumor necrosis factor, alpha, converting enzyme)	Adam17
5	NM_131911	acidic nuclear phosphoprotein 32 family, member B	Anp32b
6	NM_012912	activating transcription factor 3	Atf3
7	BM391471	activating transcription factor 5	Atf5
8	NM_019361	activity regulated cytoskeletal-associated protein	Arc
9	AI600029	activity-dependent neuroprotective protein	Adnp
10	NM_017155	adenosine A1 receptor	Adora1
11	AF228684	adenosine A2a receptor	Adora2a
12	NM_012896	adenosine A3 receptor	Adora3
13	NM_031006	adenosine deaminase, RNA-specific	Adar
14	AW523747	adhesion molecule with Ig like domain 2	Amigo2
15	U07126	adrenergic receptor, alpha 1a	Adra1c
16	AY057895	adrenergic receptor, beta 2	Adrb2
17	NM_012715	adrenomedullin	Adm
18	NM_134326	albumin	Alb
19	NM_022407	aldehyde dehydrogenase family 1, member A1	Aldh1a1
20	NM_012498	aldo-keto reductase family 1, member B4 (aldose reductase)	Akr1b4
21	NM_017196	allograft inflammatory factor 1	Aif1
22	NM_012493	alpha-fetoprotein	Afp
23	NM_012892	amiloride-sensitive cation channel 1, neuronal (degenerin)	Accn1
24	BM986220	amyloid beta (A4) precursor protein	App
25	NM_053957	amyloid beta (A4) precursor protein-binding, family B, member 3	Apbb3
26	U90829	amyloid beta precursor protein binding protein 1	Appbp1
27	NM_012502	androgen receptor	Ar
28	AF275151	androgen receptor-related apoptosis-associated protein CBL27	Cbl27
29	BI275292	angiopoietin 2	Angpt2
30	AA818262	angiopoietin-like 4	Angptl4
31	AF201331	angiotensin I converting enzyme (peptidyl-dipeptidase A) 1	Ace
32	BF552873	angiotensin II receptor, type 2	Agtr2
33	NM_031009	angiotensin receptor 1b	Agtr1b
34	NM_134432	angiotensinogen (serpin peptidase inhibitor, clade A, member 8)	Agt
35	AJ428573	ankyrin 3, epithelial	Ank3
36	L81174	ankyrin repeat domain 1 (cardiac muscle)	Ankrd1
37	NM_012904	annexin A1	Anxa1
38	NM_024155	annexin A4	Anxa4
39	NM_013132	annexin A5	Anxa5
40	BI275921	anterior pharynx defective 1a homolog (C. elegans)	Aph1a
41	NM_133400	apobec-1 complementation factor	Acf
42	J02582	apolipoprotein E	Apoe
43	NM_053720	apoptosis antagonizing transcription factor	Aatf
44	AI233249	apoptosis inhibitor 5 (predicted)	Api5_predicted
45	AW144082	Apoptosis, caspase activation inhibitor (predicted)	Aven_predicted
46	AA894233	apoptosis-inducing factor (AIF)-like mitochondrion-associated inducer of death (predicted)	Amid_predicted
47	BE116857	apoptotic chromatin condensation inducer 1	Acin1
48	AF218388	apoptotic peptidase activating factor 1	Apaf1
49	L07268	aquaporin 1	Aqp1
50	NM_019158	aquaporin 8	Aqp8
51	NM_031010	arachidonate 15-lipoxygenase	Alox15
52	BF285345	arrestin, beta 2	Arrb2
53	NM_013149	aryl hydrocarbon receptor	Ahr
54	NM_012780	aryl hydrocarbon receptor nuclear translocator	Arnt
55	NM_021590	aryl hydrocarbon receptor-interacting protein-like 1	Aipl1
56	BI274345	ataxin 10	Atxn10
57	NM_058213	ATPase, Ca++ transporting, cardiac muscle, fast twitch 1	Atp2a1
58	J04024	ATPase, Ca++ transporting, cardiac muscle, slow twitch 2	Atp2a2
59	AY082609	ATP-binding cassette, sub-family B (MDR/TAP), member 1/ ATP-binding cassette, sub-family B (MDR/TAP), member 1A	Abcb1 /// Abcb1a
60	NM_017228	atrophin 1	Atn1
61	AI169001	autophagy-related 12 (yeast)	Atg12

62	AI406520	AXL receptor tyrosine kinase	Axl
63	NM_021752	baculoviral IAP repeat-containing 2	Birc2
64	NM_023987	baculoviral IAP repeat-containing 3	Birc3
65	AF304333	baculoviral IAP repeat-containing 4	Birc4
66	NM_022274	baculoviral IAP repeat-containing 5	Birc5
67	NM_031328	B-cell CLL/lymphoma 10	Bcl10
68	NM_016993	B-cell leukemia/lymphoma 2	Bcl2
69	NM_133416	B-cell leukemia/lymphoma 2 related protein A1	Bcl2a1
70	AI172204	B-cell receptor-associated protein 29	Bcap29
71	AI409930	B-cell receptor-associated protein 31	Bcap31
72	NM_017258	B-cell translocation gene 1, anti-proliferative	Btg1
73	BI288701	B-cell translocation gene 2, anti-proliferative	Btg2
74	NM_139258	Bcl2 modifying factor	Bmf
75	NM_053420	BCL2/adenovirus E1B 19 kDa-interacting protein 3	Bnip3
76	NM_080888	BCL2/adenovirus E1B 19 kDa-interacting protein 3-like	Bnip3l
77	NM_080897	BCL2/adenovirus E1B 19kDa-interacting protein 1	Bnip1
78	AI178277	BCL2/adenovirus E1B 19kDa-interacting protein 1, NIP2 (predicted)	Bnip2_predicted
79	NM_053812	BCL2-antagonist/killer 1	Bak1
80	BI280304	Bcl2-associated athanogene 1 (predicted)	Bag1_predicted
81	AI231792	Bcl2-associated athanogene 3	Bag3
82	BI282898	BCL2-associated athanogene 5	Bag5
83	AF279911	bcl2-associated death promoter	Bad
84	AI717547	BCL2-associated transcription factor 1	Bclaf1
85	AF235993	Bcl2-associated X protein	Bax
86	U72350	Bcl2-like 1	Bcl2l1
87	NM_053733	Bcl2-like 10	Bcl2l10
88	NM_022612	BCL2-like 11 (apoptosis facilitator)	Bcl2l11
89	AI227978	BCL2-like 12 (proline rich) (predicted)	Bcl2l12_predicted
90	AA892271	BCL2-like 13 (apoptosis facilitator) (predicted)	Bcl2l13_predicted
91	NM_021850	Bcl2-like 2	Bcl2l2
92	AF051093	Bcl-2-related ovarian killer protein	Bok
93	NM_053739	beclin 1 (coiled-coil, myosin-like BCL2-interacting protein)	Becn1
94	AI008680	benzodiazepine receptor, peripheral	Bzrp
95	NM_057130	BH3 interacting (with BCL2 family) domain, apoptosis agonist	Bid3
96	AF136282	BH3 interacting domain death agonist	Bid
97	AI177631	bifunctional apoptosis regulator	Bfar
98	NM_012827	bone morphogenetic protein 4	Bmp4
99	BE118651	bone morphogenic protein receptor, type II (serine/threonine kinase)	Bmpr2
100	AA851481	brain and reproductive organ-expressed protein	Bre
101	X67108	brain derived neurotrophic factor	Bdnf
102	AI169085	brain zinc finger protein	Zfp179
103	NM_017253	branched chain aminotransferase 1, cytosolic	Bcat1
104	NM_022622	BRCA1 associated RING domain 1	Bard1
105	BF404972	Breast cancer 1	Brca1
106	NM_012931	breast cancer anti-estrogen resistance 1	Bcar1
107	NM_134413	BTB (POZ) domain containing 14B	Btbd14b
108	NM_031334	cadherin 1	Cdh1
109	NM_019161	cadherin 22	Cdh22
110	AF061947	calcineurin binding protein 1	Cabin1
111	BM958511	calcium binding protein p22	Chp
112	AB070350	calcium binding protein p22 /// similar to calcium binding protein P22 (predicted) /// similar to calcium binding protein P22 (predicted)	Chp /// RGD1565588_predicted /// RGD1564956_predicted
113	BF404381	Calcium/calmodulin-dependent protein kinase II, alpha	Chp /// RGD1565588_predicted /// RGD1564956_predicted
114	NM_016996	calcium-sensing receptor	Casr
115	NM_019152	calpain 1	Capn1
116	NM_053295	calpastatin	Cast
117	NM_022399	calreticulin	Calr
118	NM_032462	Calsenilin, presenilin binding protein, EF hand transcription factor	Csen
119	NM_031017	cAMP responsive element binding protein 1	Creb1
120	NM_017334	cAMP responsive element modulator	Crem
121	NM_012784	cannabinoid receptor 1 (brain)	Cnr1
122	AW252112	carbonic anhydrase 11	Car11
123	BF281311	casein kinase 2, beta subunit	Csnk2b

124	NM_057138	CASP8 and FADD-like apoptosis regulator	Cflar
125	D85899	caspase 1	Casp1
126	NM_130422	caspase 12	Casp12
127	AF136231	caspase 2	Casp2
128	BM387008	caspase 3, apoptosis related cysteine protease	Casp3
129	NM_053736	caspase 4, apoptosis-related cysteine peptidase	Casp4
130	NM_031775	caspase 6	Casp6
131	BF283754	caspase 7	Casp7
132	1369262_at	caspase 8	Casp8
133	BF282281	caspase 8 associated protein 2 (predicted)	Casp8ap2_predicted
134	AF262319	caspase 9	Casp9
135	NM_022303	caspase recruitment domain family, member 9	Card9
136	AI136555	castration induced prostatic apoptosis-related protein 1	Cipar1
137	NM_022597	cathepsin B	Ctsb
138	NM_134334	cathepsin D	Ctsd
139	AI548979	cationic trypsinogen	LOC286911
140	NM_024125	CCAAT/enhancer binding protein (C/EBP), beta	Cebpb
141	1368813_at	CCAAT/enhancer binding protein (C/EBP), delta	Cebpd
142	NM_021744	CD14 antigen	Cd14
143	NM_017079	CD1d1 antigen	Cd1d1
144	NM_012830	CD2 antigen	Cd2
145	NM_013121	CD28 antigen	Cd28
146	1389997_at	CD3 antigen, epsilon polypeptide (predicted)	Cd3e_predicted
147	AI044631	CD3 antigen, gamma polypeptide	Cd3g_predicted
148	D30795	CD38 antigen	Cd38
149	AF065147	CD44 antigen	Cd44
150	NM_019295	CD5 antigen	Cd5
151	NM_012523	CD53 antigen	Cd53
152	NM_013069	CD74 antigen (invariant polypeptide of major histocompatibility complex, class II antigen-associated)	Cd74
153	NM_031755	CEA-related cell adhesion molecule 1	Ceacam1
154	U23056	CEA-related cell adhesion molecule 1 /// CEA-related cell adhesion molecule 10	Ceacam1 /// Ceacam10
155	BF284899	cell death-inducing DNA fragmentation factor, alpha subunit-like effector A (predicted)	Cidea_predicted
156	L24388	cell division cycle 2 homolog (S.pombe)-like 1	Cdc2
157	AI059933	Cell division cycle 25 homolog A (S. cerevisiae)	Cdc2
158	NM_023026	centaurin, gamma 1	Ceng1a
159	NM_031530	chemokine (C-C motif) ligand 2	Ccl2
160	NM_031116	chemokine (C-C motif) ligand 5	Ccl5
161	BE095824	chemokine (C-C motif) ligand 6	Ccl6
162	AA945737	chemokine (C-X-C motif) receptor 4	Cxcr4
163	AI012221	chloride intracellular channel 1	Clic1
164	NM_012829	cholecystokinin	Cck
165	NM_012832	cholinergic receptor, nicotinic, alpha polypeptide 7	Chrna7
166	AI171615	chromosome segregation 1-like (S. cerevisiae) (predicted)	Cse1l_predicted
167	NM_013092	chymase 1, mast cell	Cma1
168	AA957183	Citron	Cit
169	BG673439	claudin 11	Cldn11
170	AF314657	clusterin	Clu
171	NM_012950	coagulation factor II (thrombin) receptor	F2r
172	NM_013057	coagulation factor III	F3
173	BM389673	cofilin 1, non-muscle	Cfl1
174	AF092207	coiled-coil domain containing 5	Ccdc5
175	U00620	colony stimulating factor 2 (granulocyte-macrophage)	Csf2
176	NM_130825	comparative gene identification transcript 94	Cgi94
177	NM_032060	complement component 3a receptor 1	C3ar1
178	NM_053619	complement component 5, receptor 1	C5r1
179	AA819870	complement component 8, beta polypeptide (mapped)	C8b
180	NM_057146	complement component 9	C9
181	AW916366	COP9 (constitutive photomorphogenic) homolog, subunit 3 (Arabidopsis thaliana)	Cops3
182	NM_031019	corticotropin releasing hormone	Crh
183	AW433973	craniofacial development protein 1	Cfdp1
184	U47922	crystallin, alpha A	Cryaa
185	NM_012935	crystallin, alpha B	Cryab
186	AF090695	CUG triplet repeat, RNA binding protein 2	Cugbp2
187	BI284428	cullin 1 (predicted)	Cul1_predicted

188	BI295890	cullin 2 (predicted)	Cul2_predicted
189	BI285751	cullin 3 (predicted)	Cul3_predicted
190	NM_022683	cullin 5	Cul5
191	X64589	cyclin B1	Ccnb1
192	AW913890	cyclin E	Ccne
193	NM_080885	cyclin-dependent kinase 5	Cdk5
194	NM_053891	cyclin-dependent kinase 5, regulatory subunit 1 (p35)	Cdk5r1
195	H31766	cyclin-dependent kinase 9 (CDC2-related kinase)	Cdk9
196	AI010427	cyclin-dependent kinase inhibitor 1A	Cdkn1a
197	AI013919	cyclin-dependent kinase inhibitor 1C (P57)	Cdkn1c
198	AF474976	cyclin-dependent kinase inhibitor 2A	Cdkn2a
199	AI409867	cystatin B	Cstb
200	BG666933	cystatin C	Cst3
201	NM_031327	cysteine rich protein 61	Cyr61
202	NM_023965	cytochrome b-245, beta polypeptide	Cybb
203	NM_012839	cytochrome c, somatic	Cycs
204	NM_012840	cytochrome c, testis	Cyct
205	NM_012840	cytochrome c, testis /// phosphodiesterase 11A	Cyctpd11
206	X00469	cytochrome P450, family 1, subfamily a, polypeptide 1	Cyp1a1
207	NM_031543	cytochrome P450, family 2, subfamily e, polypeptide 1	Cyp2e1
208	BF285068	cytokine induced apoptosis inhibitor 1	Ciapin1
209	BI298817	Cytotoxic granule-associated RNA binding protein 1	Tia1
210	AI169146	D4, zinc and double PHD fingers family 2 (predicted)	Dpf2_predicted
211	AI408110	DEAD (Asp-Glu-Ala-Asp) box polypeptide 19	Ddx19
212	BM389310	DEAD (Asp-Glu-Ala-Asp) box polypeptide 41 (predicted)	Ddx41_predicted
213	BI285645	death associated protein 3	Dap3
214	AA818353	death associated protein kinase 1 (predicted)	Dapk1_predicted
215	NM_031800	death effector domain-containing	Dedd
216	NM_022526	death-associated protein	Dap
217	NM_022546	death-associated protein kinase 3	Dapk3
218	AI013627	defender against cell death 1	Dad1
219	NM_080482	deleted in bladder cancer chromosome region candidate 1 (human)	Dbccr
220	NM_012841	deleted in colorectal carcinoma	Dcc
221	NM_013097	deoxyribonuclease I	Dnase1
222	AF178975	deoxyribonuclease II	Dnase2
223	NM_053907	deoxyribonuclease I-like 3	LOC681124
224	NM_022531	desmin	Des
225	BE110572	diablo homolog (Drosophila)	Diablo
226	AI236726	DNA fragmentation factor, alpha subunit	Dffa
227	NM_053362	DNA fragmentation factor, beta subunit	Dffb
228	NM_024134	DNA-damage inducible transcript 3	Ddit3
229	NM_080906	DNA-damage-inducible transcript 4	Ddit4
230	BI282224	DnaJ (Hsp40) homolog, subfamily A, member 3	LOC294513
231	BM384926	DnaJ (Hsp40) homolog, subfamily B, member 1 (predicted)	Dnajb1_predicted
232	NM_012699	DnaJ (Hsp40) homolog, subfamily B, member 9	Dnajb9
233	BI285682	DnaJ (Hsp40) homolog, subfamily C, member 7	Dnajc7
234	BF406540	DnaJ (Hsp40) related, subfamily B, member 13	Dnajb13
235	L12407	dopamine beta hydroxylase	Dbh
236	NM_012547	dopamine receptor 2	Drd2
237	M35077	dopamine receptor D1A	Drd1a
238	BE110108	dual specificity phosphatase 1	Dusp1
239	AI172067	dual specificity phosphatase 22 (predicted)	Dusp22_predicted
240	U23438	dual specificity phosphatase 4	Dusp4
241	NM_133578	dual specificity phosphatase 5	Dusp5
242	NM_053883	dual specificity phosphatase 6	Dusp6
243	L24562	dynamin 2	Dnm2
244	NM_053319	dynein light chain LC8-type 1	Dynll1
245	NM_012551	early growth response 1	Egr1
246	AF115249	endothelial differentiation, sphingolipid G-protein-coupled receptor, 8	Edg8
247	NM_023090	endothelial PAS domain protein 1	Epas1
248	NM_053596	endothelin converting enzyme 1	Ece1
249	AB023896	endothelin converting enzyme-like 1	Ece1l
250	X57764	endothelin receptor type B	Ednrb
251	BI291645	engulfment and cell motility 3, ced-12 homolog (C. elegans)	Elmo3
252	NM_012842	epidermal growth factor	Egf
253	M37394	epidermal growth factor receptor	Egfr

254	AF187818	epidermal growth factor receptor /// peptidase D (mapped)	Egfr /// Pepd_mapped
255	BF564277	epilepsy, progressive myoclonic epilepsy, type 2 gene alpha	Epme
256	NM_017001	erythropoietin	Epo
257	AA866269	Estrogen receptor 1	Esr1
258	AF042058	estrogen receptor 2 beta	Esr2b
259	BF398331	estrogen receptor-binding fragment-associated gene 9	Ebag9
260	AI412114	etoposide induced 2.4 mRNA	Ei24
261	NM_012660	eukaryotic translation elongation factor 1 alpha 2	Eef1a2
262	AI600237	eukaryotic translation elongation factor 1 epsilon 1 (predicted)	Eef1e1_predicted
263	NM_053950	eukaryotic translation initiation factor 2B, subunit 4 delta	Eif2b4
264	NM_053974	eukaryotic translation initiation factor 4E	Eif4e
265	BI283681	eukaryotic translation initiation factor 5A	Eif5a
266	BM388758	excision repair cross-complementing rodent repair deficiency, complementation group 3	Ercc3
267	D13374	expressed in non-metastatic cells 1	Nme1
268	AI385371	extra spindle poles like 1 (S. cerevisiae) (predicted)	Espl1_predicted
269	NM_080895	Fas apoptotic inhibitory molecule	Faim
270	AF044201	Fas apoptotic inhibitory molecule 2	Faim2
271	NM_080891	Fas death domain-associated protein	Daxx
272	NM_012908	Fas ligand (TNF superfamily, member 6)	Faslg
273	AI227743	Fas-activated serine/threonine kinase	Fastk
274	NM_130406	Fas-associated factor 1	Faf1
275	NM_053843	Fc receptor, IgG, low affinity III /// Fc gamma receptor II beta	Fcgr3 /// LOC498276
276	AA999104	Feminization 1 homolog b (C. elegans) (predicted)	Fem1_predicted
277	NM_019305	fibroblast growth factor 2	Fgf2
278	NM_130817	fibroblast growth factor 3	Fgf3
279	AB079673	fibroblast growth factor 4	Fgf4
280	NM_133286	fibroblast growth factor 8	Fgf8
281	S54008	Fibroblast growth factor receptor 1	Fgfr1
282	NM_053429	fibroblast growth factor receptor 3	Fgfr3
283	AA893484	fibronectin 1	Fn1
284	AI103600	Filamin C, gamma (actin binding protein 280) (predicted)	Flnc_predicted
285	AF040256	folate hydrolase	Folh1
286	M36804	follicle stimulating hormone beta	Fshb
287	NM_012561	follistatin	Fst
288	BI295511	forkhead box O1A	Foxo1a
289	AI231684	forkhead box O3a (predicted)	Foxo3a_predicted
290	NM_012953	fos-like antigen 1	Fosl1
291	NM_012954	fos-like antigen 2 /// FBJ osteosarcoma oncogene B	Fosl2 /// Fosb
292	NM_017181	fumarylacetoacetate hydrolase	Fah
293	BE108192	G1 to S phase transition 1	Gspt1
294	NM_033237	galanin	Gal
295	NM_019172	galanin receptor 2	Galr2
296	NM_053840	gamma-glutamyltransferase 1	Ggt1
297	NM_019281	gap junction membrane channel protein alpha 9	Gja9
298	NM_053388	gap junction membrane channel protein beta 6	Gja6
299	NM_012849	gastrin	Gast
300	AA945758	gb:AA945758 /DB_XREF=gi:3105674 /DB_XREF=EST201257 /CLONE=RLUAS87 /FEA=EST /CNT=13 /TID=Rn.7908.1 /TIER=Stack /STK=8 /UG=Rn.7908 /UG_TITLE=ESTs	NS
301	AI230220	gb:AI230220 /DB_XREF=gi:3814107 /DB_XREF=EST226915 /CLONE=REMCT79 /FEA=EST /CNT=9 /TID=Rn.24381.1 /TIER=Stack /STK=7 /UG=Rn.24381 /UG_TITLE=ESTs, Moderately similar to MLE3 RAT MYOSIN LIGHT CHAIN 3, SKELETAL MUSCLE ISOFORM (R.norvegicus)	NS
302	BF555051	gb:BF555051 /DB_XREF=gi:11664781 /DB_XREF=UI-R-E0-cg-f-04-0-UI.r1 /CLONE=UI-R-E0-cg-f-04-0-UI /FEA=EST /CNT=3 /TID=Rn.65517.1 /TIER=ConsEnd /STK=1 /UG=Rn.65517 /UG_TITLE=ESTs, Weakly similar to VITAMIN K-DEPENDENT PROTEIN S PRECURSOR (R.norvegicus)	NS
303	BM384229	gb:BM384229 /DB_XREF=gi:18184282 /DB_XREF=UI-R-DZ0-cks-c-03-0-UI.s1 /CLONE=UI-R-DZ0-cks-c-03-0-UI /FEA=EST /CNT=12 /TID=Rn.14615.1 /TIER=Stack /STK=11 /UG=Rn.14615 /UG_TITLE=ESTs, Highly similar to TRA2 MOUSE TNF RECEPTOR ASSOCIATED FACTOR 2 (M.musculus)	NS
304	J02582	gb:J02582 /DB_XREF=gi:202957 /FEA=DNA_2 /CNT=1 /TID=Rn.64667.1 /TIER=ConsEnd /STK=0 /UG=Rn.64667 /UG_TITLE=Rat apolipoprotein E gene, complete cds /DEF=Rat apolipoprotein E gene, complete cds	NS
305	BI285576	gelsolin	Gsn
306	NM_021669	ghrelin precursor	Ghrl
307	NM_019139	glial cell line derived neurotrophic factor	Gdnf
308	BF281741	glioma tumor suppressor candidate region gene 2	Gltscr2

309	NM_012728	glucagon-like peptide 1 receptor	Glp1r
310	BI283882	glucose phosphate isomerase	Gpi
311	NM_017006	glucose-6-phosphate dehydrogenase X-linked	G6pdx
312	U08259	glutamate receptor, ionotropic, NMDA2C	Grin2c
313	NM_017010	glutamate receptor, ionotropic, N-methyl D-aspartate 1	Grin1
314	AF001423	glutamate receptor, ionotropic, N-methyl D-aspartate 2A	Grin2a
315	M91562	glutamate receptor, ionotropic, N-methyl D-aspartate 2B	Grin2b
316	NM_017011	glutamate receptor, metabotropic 1	Gria2bm1
317	M92075	glutamate receptor, metabotropic 2	Grm2
318	AW522430	glutamate receptor, metabotropic 3	Grm3
319	NM_022202	glutamate receptor, metabotropic 8	Gria2bm8
320	J05181	glutamate-cysteine ligase, catalytic subunit	Gclc
321	BG380882	glutaminyl-tRNA synthetase /// similar to glutaminyl-tRNA synthetase (predicted)	Qars /// RGD1562301_predicted
322	NM_022278	glutaredoxin 1 (thioltransferase)	Glrx1
323	S41066	glutathione peroxidase 1	Gpx1
324	NM_017165	glutathione peroxidase 4	Gpx4
325	NM_017013	glutathione-S-transferase, alpha type2	Gsta2
326	X02904	glutathione-S-transferase, pi 1 /// glutathione S-transferase, pi 2	Gstp1 /// Gstp2
327	NM_017008	glyceraldehyde-3-phosphate dehydrogenase /// similar to glyceraldehyde-3-phosphate dehydrogenase (predicted) /// similar to glyceraldehyde-3-phosphate dehydrogenase (predicted) /// similar to glyceraldehyde-3-phosphate dehydrogenase (predicted) /// similar to glyceraldehyde-3-phosphate dehydrogenase (predicted)	Gapdh /// RGD1564688_predicted /// RGD1564351_predicted /// RGD1561683_predicted /// RGD1565368_predicted
328	BF287444	glycogen synthase kinase 3 beta	Gsk3b
329	AI103970	glyoxylase 1	Glo1
330	BM391371	goliath	LOC652955
331	NM_031038	gonadotropin releasing hormone receptor	Gnrhr
332	NM_012767	gonadotropin-releasing hormone 1	Gnrh1
333	M34097	granzyme B	Gzmb
334	U57063	granzyme G	Gzmg
335	NM_019282	gremlin 1 homolog, cysteine knot superfamily (Xenopus laevis)	Grem1
336	NM_024127	growth arrest and DNA-damage-inducible 45 alpha	Gadd45a
337	BI287978	growth arrest and DNA-damage-inducible 45 beta	Gadd45b
338	AI599423	growth arrest and DNA-damage-inducible 45 gamma	Gadd45g
339	NM_057100	growth arrest specific 6	Gas6
340	X62853	Growth factor receptor bound protein 2	Grb2
341	V01238	growth hormone 1	Gh1
342	AI170771	growth hormone receptor	Ghr
343	U94321	growth hormone secretagogue receptor	Gshr
344	NM_024356	GTP cyclohydrolase 1	Gch
345	BM389208	GTPase, IMAP family member 4	Gimap4
346	M12672	guanine nucleotide binding protein, alpha inhibiting 2	Gnai2
347	BE117491	guanine nucleotide binding protein, alpha q polypeptide	Gnaq
348	BM390519	GULP, engulfment adaptor PTB domain containing 1	Gulp1
349	BG379941	Harvey rat sarcoma viral (v-Ha-ras) oncogene homolog	Hras
350	NM_012966	heat shock 10 kDa protein 1 (chaperonin 10)	Hspe1
351	AI236601	heat shock 105kDa/110kDa protein 1	Hsph1
352	NM_031970	heat shock 27kDa protein 1	Hspb1
353	NM_031971	heat shock 70kD protein 1A /// heat shock 70kD protein 1B (mapped)	Hspa1a /// Hspa1b_mapped
354	BI278231	heat shock 70kD protein 1B (mapped)	Hspa1b_mapped
355	M14050	heat shock 70kDa protein 5 (glucose-regulated protein)	Hspa5
356	BI282281	heat shock 70kDa protein 9A (predicted)	Hspa9a_predicted
357	AI237389	heat shock 90kDa protein 1, beta	Hspcb
358	NM_022229	heat shock protein 1 (chaperonin)	Hspd1
359	BG671521	heat shock protein 1, alpha	Hspca
360	AF077354	heat shock protein 4	Hspa4
361	NM_012580	heme oxygenase (decycling) 1	Hmox1
362	NM_013185	hemopoietic cell kinase	Hck
363	1387701_at	hepatocyte growth factor	Hgf
364	NM_012734	hexokinase 1	Hk1
365	NM_012735	hexokinase 2	Hk2
366	BG378885	high mobility group AT-hook 1	Hmga1
367	BE107162	high mobility group box 1	Hmgb1

368	AF275734	high mobility group box 1 /// similar to High mobility group protein 1 (HMG-1) (predicted) /// similar to Hmgb1 protein (predicted) /// similar to High mobility group protein 1 (HMG-1) (predicted)	Hmgb1 /// RGD1562312_predicted /// RGD1563786_predicted /// RGD1563012_predicted
369	AI180339	histone deacetylase 1 (predicted)	Hdac1_predicted
370	NM_053448	histone deacetylase 3	Hdac3
371	BF403027	histone deacetylase 5	Hdac5
372	NM_053609	HLA-B-associated transcript 3	Bat3
373	M37568	homeo box C8 (mapped)	Hoxc8_mapped
374	BM392321	homeodomain interacting protein kinase 2 (predicted)	Hipk2_predicted
375	NM_031787	homeodomain interacting protein kinase 3	Hipk3
376	AB003726	homer homolog 1 (Drosophila)	Homer1
377	NM_053523	homocysteine-inducible, endoplasmic reticulum stress-inducible, ubiquitin-like domain member 1	Herpud1
378	BE111733	hormone-regulated proliferation associated protein 20	Hrpap20
379	AW253339	huntingtin interacting protein 1	Hip1
380	U18650	Huntington disease gene homolog	Hdh
381	NM_019371	hypothetical gene supported by NM_019371	LOC497816
382	BM390522	hypothetical gene supported by NM_130426	LOC497808
383	H31665	hypoxia induced gene 1	Hig1
384	NM_024359	hypoxia inducible factor 1, alpha subunit	Hif1a
385	BI282904	hypoxia up-regulated 1	Hyou1
386	AI176519	immediate early response 3	Ier3
387	AI411947	immunoglobulin heavy chain 1a (serum IgG2a)	Igh-1a
388	NM_023973	indoleamine-pyrrole 2,3 dioxygenase	Indo
389	NM_012590	inhibin alpha	Inha
390	NM_017128	inhibin beta-A	Inhba
391	NM_013060	inhibitor of DNA binding 2	Id2
392	AF000942	inhibitor of DNA binding 3	Id3
393	NM_053355	inhibitor of kappaB kinase beta	Ikbkb
394	J05510	inositol 1,4,5-triphosphate receptor 1	Itpr1
395	NM_019311	inositol polyphosphate-5-phosphatase D	Inppd5
396	NM_019129	insulin 1	Igf2bp1
397	NM_032074	insulin receptor substrate 3	Irs3
398	M15481	insulin-like growth factor 1	Igf1
399	NM_052807	insulin-like growth factor 1 receptor	Igf1r
400	NM_031511	insulin-like growth factor 2	Igf2
401	NM_012588	insulin-like growth factor binding protein 3	Igfbp3
402	BF282337	integral membrane protein 2B	Itm2b
403	NM_017022	integrin beta 1 (fibronectin receptor beta)	Itgb1
404	NM_133409	integrin linked kinase	Ilk
405	NM_019127	interferon beta 1, fibroblast	Ifnb1f
406	AF010466	interferon gamma	Ifng
407	NM_012591	interferon regulatory factor 1	Irf1
408	NM_017019	interleukin 1 alpha	Il1a
409	NM_031512	interleukin 1 beta	Il1b
410	L02926	interleukin 10	Il10
411	AF347936	interleukin 11 receptor, alpha chain 1	Il11ra1
412	NM_053828	interleukin 13	Il13
413	AF015718	interleukin 15	Il15
414	AJ222813	interleukin 18	Il18
415	NM_013163	interleukin 2 receptor, alpha chain	Il2ra
416	NM_013195	interleukin 2 receptor, beta chain	Il2rb
417	NM_031513	interleukin 3	Il6
418	X16058	interleukin 4	Il4
419	NM_012589	interleukin 6	Il6
420	AF367210	interleukin 7	Il7
421	BF405951	Interleukin-1 receptor-associated kinase 4 (predicted)	Irak4_predicted
422	1388184_at	isoprenylcysteine carboxyl methyltransferase	Icmt
423	NM_031514	Janus kinase 2	Jak2
424	BE096021	Jun D proto-oncogene	Jund1
425	BI288619	Jun oncogene	Jun
426	NM_021836	Jun-B oncogene	Junb
427	NM_012696	kininogen 1 /// K-kininogen /// similar to alpha-1 major acute phase protein prepeptide	Kng1 /// LOC25087 /// MGC108747

428	NM_031135	Kruppel-like factor 10	Klf10
429	BM385790	Kruppel-like factor 2 (lung) (predicted)	Klf2_predicted
430	NM_053394	Kruppel-like factor 5	Klf5
431	NM_053902	kynureninase (L-kynurenine hydrolase)	Kynu
432	NM_012594	Lactalbumin, alpha	Lalba
433	NM_019904	lectin, galactose binding, soluble 1	Lgals1
434	NM_031832	lectin, galactose binding, soluble 3	Lgals3
435	NM_022582	lectin, galactose binding, soluble 7	Lgals7
436	NM_031048	leukemia inhibitory factor receptor	Lifr
437	NM_031727	LIM motif-containing protein kinase 1	Limk1
438	NM_130741	lipocalin 2	Lcn2
439	BF289368	lipopolysaccharide binding protein	Lbp
440	BI284739	LPS-induced TN factor	Litaf
441	AA874924	lymphocyte antigen 86 (predicted)	Ly86_predicted
442	AI137137	lymphocyte protein tyrosine kinase (mapped)	Lck_mapped
443	AI012109	lymphocyte specific 1	Lsp1
444	NM_080769	lymphotoxin A	Lta
445	NM_053538	lysosomal-associated protein transmembrane 5	Laptm5
446	NM_031051	macrophage migration inhibitory factor	Mif
447	NM_024352	Macrophage stimulating 1 (hepatocyte growth factor-like)	Mst1
448	NM_019191	MAD homolog 2 (Drosophila)	Smad2
449	AA997679	MAD homolog 3 (Drosophila)	Smad3
450	NM_019275	MAD homolog 4 (Drosophila)	Smad4
451	AW521447	MAD homolog 7 (Drosophila)	Madh7
452	NM_053585	MAP-kinase activating death domain	Madd
453	U65656	matrix metallopeptidase 2	Mmp2
454	NM_031055	matrix metallopeptidase 9	Mmp9
455	BI289109	max binding protein (predicted)	Mnt_predicted
456	AW143154	megakaryoblastic leukemia (translocation) 1 (predicted)	Mkl1_predicted
457	NM_053409	melanoma antigen, family D, 1	Maged1
458	AF411318	metallothionein 1a	Mt1a
459	NM_053307	methionine sulfoxide reductase A	Msrb2
460	BI281702	microtubule-associated protein 1b	Map1b
461	BE107978	microtubule-associated protein tau /// hypothetical gene supported by NM_017212	Mapt /// LOC497674
462	BG665132	mitochondrial carrier homolog 1 (C. elegans)	Mtch1
463	AA943734	mitochondrial protein, 18 kDa	MGC94604
464	BG378230	mitochondrial ribosomal protein S30 (predicted)	Mrps30_predicted
465	NM_053842	mitogen activated protein kinase 1	Mapk1
466	NM_012806	mitogen activated protein kinase 10	Mapk10
467	AW254190	mitogen activated protein kinase 14	Mapk14
468	AF155236	mitogen activated protein kinase 3	Mapk3
469	NM_053777	mitogen activated protein kinase 8 interacting protein	Mapk8ip
470	D13341	mitogen activated protein kinase kinase 1	Map2k1
471	D14592	mitogen activated protein kinase kinase 2	Map2k2
472	NM_053887	mitogen activated protein kinase kinase kinase 1	Map3k1
473	NM_013055	mitogen activated protein kinase kinase kinase 12	Map3k12
474	AI146037	Mitogen activated protein kinase kinase kinase 7 (predicted)	Map3k7_predicted
475	AI575972	Mitogen-activated protein kinase 8 interacting protein 2	Mapk8ip2
476	NM_017322	mitogen-activated protein kinase 9	Mapk9
477	BI281589	mitogen-activated protein kinase kinase kinase 11	Map3k11
478	NM_053847	mitogen-activated protein kinase kinase kinase 8	Map3k8
479	D00688	monoamine oxidase A	Maoa
480	NM_012982	msh homeo box homolog 2 (Drosophila)	Msx2
481	NM_053337	Msx-interacting-zinc finger	Miz1
482	BI274326	mucin 1, transmembrane	Muc1
483	BM391100	mucin 4	Muc4
484	NM_031053	mutL homolog 1 (E. coli) /// hypothetical gene supported by NM_031053	Mlh1 /// LOC497834
485	NM_021837	myc-like oncogene, s-myc protein	Mycs
486	NM_012798	myelin and lymphocyte protein, T-cell differentiation protein	Mal
487	BF281184	myeloblastosis oncogene-like 2 (predicted)	Mybl2_predicted
488	NM_012603	myelocytomatosis viral oncogene homolog (avian)	Myc
489	AI172056	myeloid cell leukemia sequence 1	Mcl1
490	BI284349	myeloid differentiation primary response gene 116	Myd116
491	AI236590	myeloid differentiation primary response gene 88	Myd88
492	NM_030860	myocyte enhancer factor 2D	Mef2d

493	J02679	NAD(P)H dehydrogenase, quinone 1	Nqo1
494	NM_053683	NADPH oxidase 1	Noxa1
495	AI178285	NCK-associated protein 1	Nckap1
496	NM_031069	NEL-like 1 (chicken)	Nell1
497	NM_012610	nerve growth factor receptor (TNFR superfamily, member 16)	Ngfr
498	NM_053401	nerve growth factor receptor (TNFRSF16) associated protein 1	Ngfrap1
499	BM388972	nerve growth factor, beta (mapped)	Norb
500	U02323	neuregulin 1	Nrg1
501	NM_023968	neuropeptide Y receptor Y2	Npy2r
502	NM_021589	neurotrophic tyrosine kinase, receptor, type 1	Ntrk1
503	NM_031073	neurotrophin 3	Ntf3
504	AI598730	neurotrophin receptor associated death domain	Nradd
505	NM_053734	neutrophil cytosolic factor 1	Ncf1
506	BI285459	nicastrin	Ncstn
507	L12562	nitric oxide synthase 2, inducible	Nos2
508	AJ011116	nitric oxide synthase 3, endothelial cell	Nos3
509	NM_053507	non-metastatic cell expressed protein 3	Nme3
510	BF389398	Notch gene homolog 1 (Drosophila)	Notch1
511	AI011448	Notch gene homolog 2 (Drosophila)	Notch2
512	NM_020087	Notch gene homolog 3 (Drosophila)	Notch3
513	BG377358	nuclear factor of activated T-cells, cytoplasmic, calcineurin-dependent 4	Nfatc4
514	AA858801	nuclear factor of kappa light chain gene enhancer in B-cells 1, p105	Nfkb1
515	AW672589	nuclear factor of kappa light chain gene enhancer in B-cells inhibitor, alpha	Nfkbia
516	NM_030867	nuclear factor of kappa light chain gene enhancer in B-cells inhibitor, beta	Nfkbib
517	NM_012991	nuclear pore associated protein	Npap60
518	NM_021745	nuclear receptor subfamily 1, group H, member 4	Nr1h4
519	NM_052980	nuclear receptor subfamily 1, group I, member 2	Nrc1i2
520	NM_017323	nuclear receptor subfamily 2, group C, member 2	Nrc2c2
521	AY066016	nuclear receptor subfamily 3, group C, member 1	Nr3c1
522	NM_013131	nuclear receptor subfamily 3, group C, member 2	Nr3c2
523	NM_024388	nuclear receptor subfamily 4, group A, member 1	Nr4a1
524	NM_031628	nuclear receptor subfamily 4, group A, member 3	Nr4a3
525	NM_022799	nuclear ubiquitous casein kinase and cyclin-dependent kinase substrate	Nucks
526	NM_053516	nucleolar protein 3 (apoptosis repressor with CARD domain)	Nol3
527	NM_012992	nucleophosmin 1	Npm1
528	J04943	nucleophosmin 1 /// similar to Nucleophosmin (NPM) (Nucleolar phosphoprotein B23) (Numatrin) (Nucleolar protein NO38)	Npm1 /// LOC300303
529	BI286040	nucleoporin 62	Nup62
530	NM_133525	Nucleoside 2-deoxyribosyltransferase domain containing protein RGD620382	RGD620382
531	NM_012861	O-6-methylguanine-DNA methyltransferase	Mgmt
532	L20684	opioid receptor, mu 1	Oprl1
533	NM_133585	optic atrophy 1 homolog (human)	Opa1
534	NM_053288	orosomucoid 1	Orm1
535	NM_130402	osteoclast inhibitory lectin	Ocil
536	NM_133306	oxidized low density lipoprotein (lectin-like) receptor 1	Oldlr1
537	NM_019210	p21 (CDKN1A)-activated kinase 3	Pak3
538	NM_053289	pancreatitis-associated protein	Pap
539	NM_017044	parathyroid hormone	Pth
540	BI281756	Parkinson disease (autosomal recessive, early onset) 7	Park7
541	BG673589	paxillin	Pxn
542	AI009656	PEF protein with a long N-terminal hydrophobic domain	Peflin
543	BI291292	peptidylprolyl isomerase C	Ppic
544	AA957342	peptidylprolyl isomerase D (cyclophilin D)	Ppid
545	U68544	peptidylprolyl isomerase F (cyclophilin F)	Ppif
546	NM_017330	perforin 1 (pore forming protein)	Prf1
547	NM_017169	peroxiredoxin 2	Prdx2
548	NM_013196	peroxisome proliferator activated receptor alpha	Ppara
549	U75918	Peroxisome proliferator activated receptor delta	Ppard
550	NM_013124	peroxisome proliferator activated receptor gamma	Pparg
551	AI598971	PERP, TP53 apoptosis effector (predicted)	Perp_predicted
552	NM_021657	PH domain and leucine rich repeat protein phosphatase	Phlpp
553	NM_031606	phosphatase and tensin homolog	Pten
554	NM_053923	phosphatidylinositol 3-kinase, C2 domain containing, gamma polypeptide	Pik3ca
555	BI290699	phosphatidylinositol 3-kinase, catalytic, alpha polypeptide	Pik3ca
556	D64048	phosphatidylinositol 3-kinase, regulatory subunit, polypeptide 1	Pik3r1
557	NM_022185	phosphatidylinositol 3-kinase, regulatory subunit, polypeptide 2	Pik3r2

558	AI232697	phosphatidylserine receptor	Ptdsr
559	AI454840	Phosphodiesterase 1A, calmodulin-dependent	Pde1a
560	AF327906	phosphodiesterase 1B, Ca2+calmodulin dependent	Pde1b
561	NM_022958	phosphoinositide-3-kinase, class 3	Pik3c3
562	NM_133551	phospholipase A2, group IVA (cytosolic, calcium-dependent)	Pla2g4a
563	U51898	phospholipase A2, group VI	Pla2g6
564	U69550	phospholipase D1	Pld1
565	BE112895	phosphoprotein enriched in astrocytes 15	Pea15
566	NM_053491	plasminogen	Plg
567	NM_013151	plasminogen activator, tissue	Plat
568	NM_013085	plasminogen activator, urokinase	Plau
569	AF007789	plasminogen activator, urokinase receptor	Plaur
570	BE100812	platelet derived growth factor, alpha	Pdgfa
571	BM392366	platelet-activating factor acetylhydrolase, isoform 1b, alpha2 subunit	Pafah1b2
572	AI009219	Pleckstrin homology domain containing, family A member 5	Plekha5
573	NM_017180	pleckstrin homology-like domain, family A, member 1	Phlda1
574	NM_012760	pleiomorphic adenoma gene-like 1	Plagl1
575	AB019366	poly (ADP-ribose) glycohydrolase	Parp1
576	NM_013063	poly (ADP-ribose) polymerase family, member 1	Parp1
577	NM_017141	polymerase (DNA directed), beta	Polb
578	AW531224	polymerase (RNA) II (DNA directed) polypeptide A (mapped)	Polr2a_mapped
579	AW435212	potassium channel, subfamily K, member 3	Kcnk3
580	NM_053405	potassium channel, subfamily K, member 9	Kcnk9
581	NM_013186	potassium voltage gated channel, Shab-related subfamily, member 1	Kcnb1
582	BM385544	presenilin 1	Psen1
583	AB004454	presenilin 2	Psen2
584	AI232272	presenilin enhancer 2 homolog (C. elegans)	Psenen
585	BI278802	prion protein	Prnp
586	U05989	PRKC, apoptosis, WT1, regulator	Pawr
587	BI285575	procollagen, type 1, alpha 1	Col1a1
588	BE108058	procollagen, type XVIII, alpha 1	Col18a1
589	AI599419	Progesterone receptor	Pgr
590	AI704628	programmed cell death 2	Pdcd2
591	NM_022265	programmed cell death 4	Pdcd4
592	BF408447	programmed cell death 5 (predicted)	Pdcd5_predicted
593	BI296393	programmed cell death 6 (predicted)	Pdcd6_predicted
594	BE328942	programmed cell death 6 interacting protein	Pdcd6ip
595	AF262320	programmed cell death 8	Pdcd8
596	AI013847	programmed cell death protein 7 (predicted)	Pdcd7_predicted
597	BI282863	prohibitin	Phb
598	NM_012629	prolactin	Prl
599	L48060	prolactin receptor	Prlr
600	BI290159	proline-serine-threonine phosphatase-interacting protein 1 (predicted)	Pstpip1_predicted
601	NM_138857	prominin 2	Prom2
602	NM_031644	prostaglandin D2 synthase 2	Ptgds2
603	U03389	prostaglandin-endoperoxide synthase 2	Ptgs2
604	AI600136	protease, serine, 25	Prss25
605	NM_031978	proteasome (prosome, macropain) 26S subunit, non-ATPase, 1	Psmd1
606	NM_130430	proteasome (prosome, macropain) 26S subunit, non-ATPase, 9	Psmd9
607	NM_012803	protein C	Prc
608	AI639478	protein disulfide isomerase associated 2 (predicted)	Pdia2_predicted
609	NM_017319	protein disulfide isomerase associated 3	Pdia3
610	BF415343	protein kinase C, alpha	Prkca
611	X04440	protein kinase C, beta 1	Prkcb1
612	NM_133307	protein kinase C, delta	Prkcd
613	AA799421	protein kinase C, epsilon	Prkce
614	1370197_a_at	protein kinase C, zeta	Prkcz
615	NM_019142	protein kinase, AMP-activated, alpha 1 catalytic subunit	Prkaa1
616	NM_023991	protein kinase, AMP-activated, alpha 2 catalytic subunit	Prkaa2
617	NM_013012	protein kinase, cGMP-dependent, type II	Prkg2
618	BF400782	protein kinase, DNA activated, catalytic polypeptide (predicted)	Prkdc_predicted
619	NM_019335	Protein kinase, interferon-inducible double stranded RNA dependent	Prkr
620	NM_031527	protein phosphatase 1, catalytic subunit, alpha isoform	Ppp1ca
621	NM_013065	protein phosphatase 1, catalytic subunit, beta isoform	Ppp1cb
622	NM_022676	protein phosphatase 1, regulatory (inhibitor) subunit 1A	Ppp1rA
623	AI172276	protein phosphatase 1, regulatory (inhibitor) subunit 2	Ppp1r2

624	AB023634	protein phosphatase 1F (PP2C domain containing)	Ppm1f
625	BF408792	protein phosphatase 2 (formerly 2A), catalytic subunit, alpha isoform	Ppp2ca
626	NM_017040	protein phosphatase 2 (formerly 2A), catalytic subunit, beta isoform	Ppp2cb
627	AA800669	protein phosphatase 2 (formerly 2A), regulatory subunit A (PR 65), alpha isoform	Ppp2r1a
628	1373959_at	protein phosphatase 2 (formerly 2A), regulatory subunit A (PR 65), beta isoform	Ppp2r1b
629	AI717081	protein phosphatase 2 (formerly 2A), regulatory subunit B (PR 52), alpha isoform	Ppp2r2a
630	BE113127	Protein phosphatase 3, catalytic subunit, alpha isoform	Ppp3ca
631	NM_031729	protein phosphatase 5, catalytic subunit	Ppp5c
632	U06230	protein S (alpha)	Pros1
633	U69109	protein tyrosine kinase 2 beta	Ptk2b
634	NM_012637	protein tyrosine phosphatase, non-receptor type 1	Ptpn1
635	AI172465	Protein tyrosine phosphatase, non-receptor type 11	Ptpn11
636	NM_053908	protein tyrosine phosphatase, non-receptor type 6	Ptpn6
637	M10072	protein tyrosine phosphatase, receptor type, C	Ptprc
638	NM_022925	protein tyrosine phosphatase, receptor type, Q /// hypothetical gene supported by NM_022925; NM_198323	Ptprq
639	AI178772	prothymosin alpha	Ptma
640	NM_017034	proviral integration site 1	Pim1
641	BI294798	PTK2 protein tyrosine kinase 2	Ptk2
642	AF231010	purinergic receptor P2X, ligand-gated ion channel, 1	P2rx1
643	AF020757	purinergic receptor P2X, ligand-gated ion channel, 2	P2rx2
644	NM_019256	purinergic receptor P2X, ligand-gated ion channel, 7	P2rx7
645	NM_017255	purinergic receptor P2Y, G-protein coupled 2	P2ry2
646	BI282953	PYD and CARD domain containing	Pycard
647	NM_013018	RAB3A, member RAS oncogene family	Rab3a
648	U70777	rabaptin, RAB GTPase binding effector protein 1	Rabep1
649	AJ249986	Rap guanine nucleotide exchange factor (GEF) 1	Rapgef1
650	AF002251	Ras association (RalGDS/AF-6) domain family 5	Rassf5
651	AF081196	RAS guanyl releasing protein 1	Rasgrp2
652	AI408053	ras homolog gene family, member A	Rhoa
653	NM_022542	ras homolog gene family, member B	Rhob
654	NM_013135	RAS p21 protein activator 1	Rasa1
655	BF414025	Ras-induced senescence 1	Ris1
656	AA799542	Ras-related C3 botulinum toxin substrate 1	Rac1
657	AF036537	receptor-interacting serine-threonine kinase 3	Ripk3
658	NM_012641	regenerating islet-derived 1	Reg1
659	L20869	regenerating islet-derived 3 gamma	Reg3g
660	NM_031546	regucalcin	Rgn
661	AJ299017	ret proto-oncogene	Ret
662	AF051335	reticulon 4	Rtn4
663	AI178012	retinoblastoma 1	Rb1
664	NM_031094	retinoblastoma-like 2	Rbl2
665	NM_031528	retinoic acid receptor, alpha	Rara
666	BF419646	retinoic acid receptor, beta	Rarb
667	BI285959	retinoid X receptor alpha	Rxra
668	AI408677	Rho GDP dissociation inhibitor (GDI) alpha	Arhgdia
669	NM_031098	Rho-associated coiled-coil forming kinase 1	Rock1
670	NM_013022	Rho-associated coiled-coil forming kinase 2	Rock2
671	NM_022510	ribosomal protein L4	Rpl4
672	BI282255	ribosomal protein S5	Rps5
673	M57428	ribosomal protein S6 kinase, polypeptide 1	Rps6kb1
674	AI179991	ring finger protein 34	Rnf34
675	AA858518	ring finger protein 7 (predicted)	Rnf7_predicted
676	AI175966	Rous sarcoma oncogene	Src
677	BF403180	Runt related transcription factor 2	Runx2
678	NM_012618	S100 calcium-binding protein A4	S100a4
679	NM_013191	S100 protein, beta polypeptide	S100b
680	AA850867	sarcoglycan, gamma (dystrophin-associated glycoprotein)	Sgcg
681	NM_031541	scavenger receptor class B, member 1	Scarb1
682	BI294932	SCF apoptosis response protein 1	LOC499941
683	NM_053687	schlafen 3	Slfn3
684	BF394953	SDA1 domain containing 1	Sdad1
685	NM_019364	sec1 family domain containing 1	Scfd1
686	AF220608	secreted frizzled-related protein 4	Sfrp4
687	AB001382	secreted phosphoprotein 1	Spp1
688	NM_017310	sema domain, immunoglobulin domain (Ig), short basic domain, secreted,	Sema3a

		(semaphorin) 3A	
689	BI299759	sema domain, transmembrane domain (TM), and cytoplasmic domain, (semaphorin) 6A (predicted)	Sema6a_predicted
690	NM_133291	seminal vesicle antigen-like 2	Sval2
691	M25590	seminal vesicle protein 4	Svp4
692	BG663093	sequestosome 1	Sqstm1
693	NM_012620	serine (or cysteine) peptidase inhibitor, clade E, member 1	Serpine1
694	NM_021696	serine (or cysteine) proteinase inhibitor, clade B, member 2	Serpinb2
695	AA944455	serine incorporator 3	Serinc3
696	NM_133392	serine/threonine kinase 17b (apoptosis-inducing)	Stk17b
697	NM_019349	serine/threonine kinase 2	Stk2
698	NM_031735	serine/threonine kinase 3 (STE20 homolog, yeast)	Stk3
699	AF388527	Serpine1 mRNA binding protein 1	Serbp1
700	NM_017170	serum amyloid P-component	Apcs
701	NM_019232	serum/glucocorticoid regulated kinase	Sgk
702	NM_080905	seven in absentia 1A	Siah1a
703	NM_134457	seven in absentia 2	Siah2
704	NM_012650	sex hormone binding globulin	Shbg
705	BF284481	SH3-domain GRB2-like B1 (endophilin)	Sh3glb1
706	AF255888	SH3-domain kinase binding protein 1	Sh3kbp1
707	BF550890	sialophorin	Spn
708	NM_032612	signal transducer and activator of transcription 1	Stat1
709	BI285863	signal transducer and activator of transcription 3	Stat3
710	NM_017064	signal transducer and activator of transcription 5A	Stat5a
711	AI177626	signal transducer and activator of transcription 5B	Stat5b
712	BE110607	similar to apoptosis related protein APR-3; p18 protein (predicted)	RGD1311605_predicted
713	BF396386	similar to cell division cycle and apoptosis regulator 1 (predicted)	RGD1560358_predicted
714	BI296385	similar to chemokine (C-X-C motif) ligand 16	Cxcl16
715	BI294745	similar to livin inhibitor of apoptosis isoform beta (predicted)	RGD1562883_predicted
716	NM_021846	similar to MAP/microtubule affinity-regulating kinase 4 (MAP/microtubule affinity-regulating kinase like 1) (predicted)	RGD1561096_predicted
717	AA848545	similar to programmed cell death 10	MGC72992
718	BF282636	similar to RIKEN cDNA 1700023M03	RGD1305457
719	AW254416	Similar to TGF-beta induced apoptosis protein 12 (predicted)	RGD1308916_predicted
720	AA946199	snail homolog 1 (Drosophila)	Snai1
721	X89383	SNF related kinase	Snrk
722	NM_012647	sodium channel, voltage-gated, type 2, alpha 1 polypeptide	Scn2a
723	NM_013178	sodium channel, voltage-gated, type IV, alpha polypeptide	Snc4a
724	BI284218	solute carrier family 2 (facilitated glucose transporter), member 1	Slc2a1
725	NM_017102	solute carrier family 2 (facilitated glucose transporter), member 3	Slc2a3
726	NM_017223	solute carrier family 20, member 2	Slc20a2
727	BG666999	solute carrier family 25 (mitochondrial carrier; adenine nucleotide translocator), member 4	Slc25a4
728	NM_017206	solute carrier family 6 (neurotransmitter transporter, taurine), member 6	Slc6a6
729	NM_053442	solute carrier family 7 (cationic amino acid transporter, y+ system), member 8 /// synaptic Ras GTPase activating protein 1 homolog (rat)	Slc7a8 /// Syngap1
730	U04933	solute carrier family 8 (sodium/calcium exchanger), member 1	Slc7a8 /// Syngap1
731	NM_133522	somatostatin receptor 3 /// hypothetical gene supported by NM_133522	SSTR
732	BI275248	Son cell proliferation protein	Son
733	NM_017221	sonic hedgehog homolog (Drosophila)	Shh
734	NM_012655	Sp1 transcription factor	Sp1
735	AB049572	sphingosine kinase 1	Sphk1
736	BM386306	sphingosine kinase 2	Sphk2
737	AI169638	sphingosine-1-phosphate phosphatase 1	Sgpp1
738	U53883	ST8 alpha-N-acetyl-neuraminide alpha-2,8-sialyltransferase 1	St8sia2
739	AY083159	Stam binding protein	Stambp
740	BM386683	stanniocalcin 1	Stc1
741	NM_022230	stanniocalcin 2	Stc2
742	NM_017166	stathmin 1	Stmn1
743	AF335281	STEAP family member 3	Steap3
744	AI235465	steroid sensitive gene 1	Ssg1
745	AI009817	succinate dehydrogenase complex, subunit C, integral membrane protein	Sdhc
746	NM_134378	sulfatase 1	Sdhc
747	NM_017050	superoxide dismutase 1	Sod1
748	BG671549	superoxide dismutase 2, mitochondrial	Sod2
749	NM_058208	suppressor of cytokine signaling 2	Socs2
750	NM_053565	suppressor of cytokine signaling 3	Socs3
751	BM390864	survival motor neuron domain containing 1	Smndc1

752	AI170385	SWI/SNF related, matrix associated, actin dependent regulator of chromatin, subfamily a, member 2	Smarca2
753	BE329013	SWI/SNF related, matrix associated, actin dependent regulator of chromatin, subfamily a, member 4	Smarca4
754	NM_053442	synaptic Ras GTPase activating protein 1 homolog (rat)	Syngap1
755	NM_013026	syndecan 1	Sdc1
756	AA946430	synovial apoptosis inhibitor 1, synoviolin	Syvn1
757	NM_019169	synuclein, alpha	Snca
758	BG671061	tachykinin 1	Tac1
759	BM392226	TAF10 RNA polymerase II, TATA box binding protein (TBP)-associated factor (predicted)	Taf10_predicted
760	NM_133615	TAF9-like RNA polymerase II, TATA box binding protein (TBP)-associated factor, 31kDa	Taf9l
761	AI228250	Tax1 (human T-cell leukemia virus type I) binding protein 1	Tax1bp1
762	AA957545	T-box 3	Tbx3
763	AB029495	TCF3 (E2A) fusion partner	Tfpt
764	AF247818	telomerase reverse transcriptase	Tert
765	NM_019381	testis enhanced gene transcript	Tegt
766	NM_133396	testis-specific kinase 2	Tesk2
767	AA943723	THAP domain containing, apoptosis associated protein 3 (predicted)	Thap3_predicted
768	NM_053800	thioredoxin 1	Txn1
769	AA800180	thioredoxin 2	Txn2
770	BM390196	thioredoxin domain containing 5 (predicted)	Txndc5_predicted
771	BF555110	thioredoxin-like 1	Txnl1
772	BM384228	THO complex 1	Thoc1
773	AA998057	thymoma viral proto-oncogene 1	Akt1
774	AI105076	Thymoma viral proto-oncogene 2	Akt2
775	NM_031575	thymoma viral proto-oncogene 3	Akt3
776	AI145313	thymus cell antigen 1, theta	Thy1
777	NM_012888	thyroid stimulating hormone receptor	Tshr
778	AI101391	Tial1 cytotoxic granule-associated RNA binding protein-like 1 (mapped)	Tial1
779	NM_053819	tissue inhibitor of metalloproteinase 1	Timp1
780	NM_021989	tissue inhibitor of metalloproteinase 2	Timp2
781	NM_012886	Tissue inhibitor of metalloproteinase 3 (Sorsby fundus dystrophy, pseudoinflammatory)	Timp3
782	AI104533	titin	Ttn
783	BI287742	TM2 domain containing 1 (predicted)	Tm2d1_predicted
784	BM389034	TNF receptor-associated protein 1	Trap1
785	BM386846	TNFRSF1A-associated via death domain	Tradd
786	AF057025	toll-like receptor 4	Tlr4
787	AI012419	Transcribed locus	NS
788	AW533194	Transcribed locus	NS
789	AI104523	Transcribed locus	NS
790	AW251860	transcription factor 7, T-cell specific (predicted)	Tcf7_predicted
791	NM_031326	transcription factor A, mitochondrial	Tfam
792	BI284455	transcription factor Pur-beta	pur-beta
793	NM_133317	transducer of ErbB-2.1	Tob1
794	M58040	transferrin receptor	Tfrc
795	BI297236	Transformation related protein 53 inducible nuclear protein 1	Trp53inp2
796	AJ277449	transformation related protein 63	Trp63
797	NM_012671	transforming growth factor alpha	Tgfa
798	AW254561	transforming growth factor beta regulated gene 4	Tbrg4
799	1370082_at	transforming growth factor, beta 1	Tgfb1
800	BF420705	transforming growth factor, beta 2	Tgfb2
801	NM_012775	transforming growth factor, beta receptor 1	Tgfbr1
802	BI275994	transglutaminase 2, C polypeptide	Tgm2
803	AB015231	transient receptor potential cation channel, subfamily V, member 1	Trpv1
804	NM_023970	transient receptor potential cation channel, subfamily V, member 4 /// transient receptor potential cation channel, subfamily V, member 1	Trpv4
805	AB020967	tribbles homolog 3 (Drosophila)	Trib3
806	NM_080903	tripartite motif protein 63	Trim63
807	AI104913	tropomodulin 1	Tmod1
808	NM_031345	TSC22 domain family 3	Tsc22d3
809	BI285434	tubulin, alpha 1 /// tubulin, alpha 6 /// similar to Tubulin alpha-2 chain (Alpha-tubulin 2) (predicted)	Tuba1 /// Tuba6 /// RGD1565476_predicted
810	BI285434	tubulin, gamma 1	Tubg1
811	AA819227	tumor necrosis factor (TNF superfamily, member 2)	Tnf
812	BF283688	tumor necrosis factor ligand superfamily member 12	Tnfsf12

813	NM_012870	tumor necrosis factor receptor superfamily, member 11b (osteoprotegerin)	Tnfrsf11b
814	BI303379	tumor necrosis factor receptor superfamily, member 12a	Tnfrsf12a
815	AI169601	tumor necrosis factor receptor superfamily, member 14 (herpesvirus entry mediator)	Tnfrsf14
816	NM_013091	tumor necrosis factor receptor superfamily, member 1a	Tnfrsf1a
817	NM_013049	tumor necrosis factor receptor superfamily, member 4	Tnfrsf4
818	AW433947	tumor necrosis factor receptor superfamily, member 5	Tnfrsf5
819	NM_139194	Tumor necrosis factor receptor superfamily, member 6	Tnfrsf6
820	BM387084	tumor necrosis factor superfamily, member 5-induced protein 1 (predicted)	Tnfsf5ip1_predicted
821	AY009504	tumor protein p53	Tp53
822	NM_053867	tumor protein, translationally-controlled 1	Tpt1
823	BG057543	tumor rejection antigen gp96 (predicted)	Tra1_predicted
824	AI234654	tumor susceptibility gene 101	Tsg101
825	NM_013052	tyrosine 3-monooxygenase/tryptophan 5-monooxygenase activation protein, eta polypeptide	Ywhah
826	NM_019376	tyrosine 3-monooxygenase/tryptophan 5-monooxygenase activation protein, gamma polypeptide	Ywhag
827	BF281342	tyrosine 3-monooxygenase/tryptophan 5-monooxygenase activation protein, theta polypeptide	Ywhaq
828	AI228292	tyrosine hydroxylase	Th
829	AI407490	tyrosyl-tRNA synthetase	Yars
830	NM_053747	Ubiquilin 1	Ubqln1
831	BI276086	Ubiquitin specific protease 7 (herpes virus-associated)	Usp7
832	BI296848	ubiquitination factor E4B, UFD2 homolog (S. cerevisiae) (predicted)	Ube4b_predicted
833	AI102437	ubiquitin-like 1 (sentrin) activating enzyme E1B	Uble1b
834	AF159706	unc-13 homolog B (C. elegans)	Unc13b
835	NM_022206	unc-5 homolog A (C. elegans)	Unc5a
836	NM_022207	unc-5 homolog B (C. elegans)	Unc5b
837	BM388453	uncharacterized protein family UPF0227 member RGD1359682	RGD1359682
838	U30789	upregulated by 1,25-dihydroxyvitamin D-3	Txnip
839	NM_053864	valosin-containing protein	Vcp
840	AF080594	vascular endothelial growth factor A	Vegfa
841	NM_012759	vav 1 oncogene	Vav1
842	NM_021687	v-erb-a erythroblastic leukemia viral oncogene homolog 4 (avian)	Erbb4
843	NM_017003	v-erb-b2 erythroblastic leukemia viral oncogene homolog 2, neuro/glioblastoma derived oncogene homolog (avian)	Erbb2
844	NM_012555	v-ets erythroblastosis virus E26 oncogene homolog 1 (avian)	Ets1
845	NM_031140	vimentin	Vim
846	AF268467	voltage-dependent anion channel 1	Vdac1
847	NM_012639	v-raf-1 murine leukemia viral oncogene homolog 1	Raf1
848	BF283772	v-rel reticuloendotheliosis viral oncogene homolog A (avian)	Rela
849	NM_022548	wild-type p53-induced gene 1	Wig1
850	NM_031534	Wilms tumor 1	Wt1
851	NM_031590	WNT1 inducible signaling pathway protein 2	Wisp2
852	BI300732	WW domain-containing oxidoreductase (predicted)	RGD1565791_predicted
853	BI282111	Y box protein 1 related, pseudogene 3 /// similar to nuclease sensitive element binding protein 1 (predicted) /// Y box protein 1	Ybx1-ps3 /// RGD1560265_predicted /// Ybx1
854	NM_031615	zinc finger protein 148	Zfp148
855	BE109605	zinc finger protein 162	Zfp162
856	BE111799	Zinc finger protein 346 (predicted)	Zfp346_predicted
857	BM392399	zinc finger protein 622	Zfp622
858	AA819804	Zinc finger protein 91	Zfp91
859	BI289543	zinc finger, MYND domain containing 11	Zmynd11
860	AI317860	zinc responsive protein ZD7	LOC474154

* Signal detected above background for gene probeset in 20% or more of the chips.
† "Yes" indicates significant differential gene expression within the Sham, SBR50, SBR50/IL-6, and SBR50/IL-6/G groups using False Discovery Rate (FDR) = 10%. "No" indicates not significant differential gene expression. "N/A" indicates genes not included in the analysis because of not being detected in at least 20% of the chips. "NS" indicates no gene symbol.

Table 2. Apoptosis-related genes differentially expressed in the SBR50 vs. SHAM comparison

mRNA Probeset Number	Gene Name*	Gene Symbol	SBR50 vs. Sham		SBR50/IL-6 vs. SBR50		SBR50/IL-6/G vs. SBR50/IL-6	
			Fold P/Sham	FDR†	Fold IL-6/P	FDR†	Fold G/IL-6	FDR†
GROUP IA GENES INCREASED IN SBR50 vs. SHAM AND DECREASED IN SBR50/IL-6 vs. SBR50								
NM_012620	serine (or cysteine) peptidase inhibitor, clade E, member 1	Serpine1	29.09	0.000	0.25	0.004	1.73	0.147
BI284218	solute carrier family 2 (facilitated glucose transporter), member 1	Slc2a1	20.29	0.000	0.26	0.002	1.72	0.079
NM_012580	heme oxygenase (decycling) 1	Hmox1	19.97	0.002	0.13	0.020	1.20	0.846
M58040	transferrin receptor	Tfrc	10.82	0.000	0.39	0.044	1.07	0.899
D64048	phosphatidylinositol 3-kinase, regulatory subunit, polypeptide 1	Pik3r1	6.17	0.003	0.21	0.014	0.64	0.433
U02315	neuregulin 1	Nrg1	5.08	0.002	0.43	0.062	0.70	0.428
NM_017334	cAMP responsive element modulator	Crem	3.81	0.001	0.59	0.079	0.57	0.078
AI172056	myeloid cell leukemia sequence 1	Mcl1	3.43	0.001	0.46	0.019	0.87	0.669
NM_080902	hypoxia induced gene 1	Hig1	3.32	0.001	0.36	0.005	1.09	0.773
AF279286	Bcl2-like 1	Bcl2l1	3.23	0.001	0.40	0.007	1.36	0.300
BI290699	phosphatidylinositol 3-kinase, catalytic, alpha polypeptide	Pik3ca	3.18	0.000	0.31	0.002	0.90	0.692
NM_019142	protein kinase, AMP-activated, alpha 1 catalytic subunit	Prkaa1	3.08	0.000	0.42	0.004	1.12	0.657
L06238	platelet derived growth factor, alpha	Pdgfa	3.00	0.002	0.43	0.015	1.05	0.885
U69550	phospholipase D1	PlaD1	2.72	0.000	0.54	0.009	0.98	0.945
AB001382	secreted phosphoprotein 1	Spp1	2.67	0.013	0.45	0.048	2.08	0.077
NM_013052	tyrosine 3-monooxygenase/tryptophan 5-monooxygenase activation protein, eta polypeptide	Ywhah	2.42	0.002	0.66	0.095	2.95	0.001
NM_053843	Fc receptor, IgG, low affinity III /// Fc gamma receptor II beta	Fcgr3	2.37	0.002	0.52	0.019	1.67	0.058
NM_017039	protein phosphatase 2 (formerly 2A), catalytic subunit, alpha isoform	Ppp2ca	2.33	0.001	0.59	0.018	1.76	0.015
BE113920	signal transducer and activator of transcription 3	Stat3	2.33	0.086	0.38	0.068	1.57	0.395
NM_019376	tyrosine 3-monooxygenase/tryptophan 5-monooxygenase activation protein, gamma polypeptide	Ywhag	2.30	0.000	0.57	0.004	1.35	0.059
NM_053887	mitogen activated protein kinase kinase kinase 1	Map3k1	2.24	0.036	0.38	0.022	1.19	0.686
NM_031140	Vimentin	Vim	2.19	0.001	0.51	0.004	1.66	0.018
NM_031514	Janus kinase 2	Jak2	2.18	0.017	0.49	0.037	0.96	0.917
NM_031832	lectin, galactose binding, soluble 3	Lgals3	2.03	0.066	0.46	0.061	2.58	0.033
NM_019232	serum/glucocorticoid regulated kinase	Sgk	2.00	0.080	0.47	0.074	0.94	0.902
AI409867	cystatin B	CstB	1.89	0.002	0.55	0.007	1.41	0.080
NM_017255	purinergic receptor P2Y, G-protein coupled 2	P2ry1	1.82	0.006	0.49	0.005	1.46	0.082
NM_017022	integrin beta 1 (fibronectin receptor beta)	Itgb1	1.82	0.001	0.61	0.006	1.15	0.351
NM_012886	tissue inhibitor of metalloproteinase 3 (Sorsby fundus dystrophy, pseudoinflammatory)	Timp3	1.80	0.022	0.64	0.093	0.95	0.859
AI600237	eukaryotic translation elongation factor 1 epsilon 1 (predicted)	Eef1e1	1.79	0.008	0.67	0.061	0.72	0.135
AF228684	adenosine A2a receptor	Adora2a	1.76	0.006	0.60	0.016	1.93	0.005
BE108192	G1 to S phase transition 1	Gspt1	1.74	0.000	0.70	0.004	1.03	0.772
NM_053619	complement component 5, receptor 1	C5r1	1.73	0.003	0.51	0.004	1.84	0.004
BI285434	tubulin, alpha 1 /// tubulin, alpha 6 /// similar to Tubulin alpha-2 chain (Alpha-tubulin 2) (predicted)	Tuba1	1.73	0.002	0.62	0.010	1.65	0.008
BM385544	presenilin 1	Psen1	1.67	0.008	0.65	0.029	1.80	0.008
BF281342	tyrosine 3-monooxygenase/tryptophan 5-monooxygenase activation protein, theta polypeptide	Ywhaq	1.63	0.001	0.69	0.009	1.09	0.463
NM_021989	tissue inhibitor of metalloproteinase 2	Timp2	1.56	0.002	0.68	0.009	0.82	0.135
AI236590	myeloid differentiation primary response gene 88	Myd88	1.56	0.044	0.56	0.019	1.30	0.272
BM392321	Homeodomain interacting protein kinase 2 (predicted)	Hipk2_predicted	1.53	0.026	0.69	0.068	0.88	0.534
BG379941	Harvey rat sarcoma viral (v-Ha-ras) oncogene homolog	Hras	1.52	0.003	0.73	0.025	1.28	0.079

BF417479	24-dehydrocholesterol reductase	Dhcr24	1.51	0.015	0.69	0.038	0.63	0.018
NM_017141	polymerase (DNA directed), beta	Polb	1.51	0.075	0.61	0.048	1.46	0.134
NM_031787	Homeodomain interacting protein kinase 3	Hipk3	1.50	0.093	0.52	0.019	0.59	0.060
AA893484	fibronectin 1	Fank1	1.49	0.028	0.64	0.022	0.74	0.116
AI172276	protein phosphatase 1, regulatory (inhibitor) subunit 2	Ppp1r2	1.47	0.008	0.79	0.092	1.06	0.727
NM_053720	apoptosis antagonizing transcription factor	Aatf	1.46	0.070	0.58	0.021	1.17	0.490
M37394	epidermal growth factor receptor	Egfr	1.44	0.092	0.52	0.012	0.52	0.014
BG666933	cystatin C	CstC	1.40	0.002	0.77	0.014	0.71	0.004
BM389673	cofilin 1, non-muscle	Cfl1	1.39	0.086	0.61	0.021	1.33	0.171
BE111972	transforming growth factor, beta receptor 1	Tgfbr1	1.37	0.090	0.63	0.027	0.92	0.680
AF388527	Serpine1 mRNA binding protein 1	Serbp1	1.31	0.016	0.83	0.096	1.11	0.365
NM_013135	RAS p21 protein activator 1	Rasa1	1.28	0.033	0.66	0.005	1.04	0.771
BI282863	Prohibitin	Phb	1.26	0.092	0.76	0.069	0.70	0.026
BI282281	heat shock 70kDa protein 9A (predicted)	Hspa9a_predicted	1.22	0.012	0.73	0.004	0.75	0.004
AI103616	ras-related C3 botulinum toxin substrate 1	Rac1	1.21	0.029	0.74	0.007	1.31	0.012
NM_019371	*EGL nine homolog 3*	*Egln3*	*17.30*	*0.000*	*0.07*	*0.000*	*0.81*	*0.493*
AI602811	*dual specificity phosphatase 6*	*Dusp6*	*13.48*	*0.000*	*0.44*	*0.012*	*1.27*	*0.418*
BI303379	*tumor necrosis factor receptor superfamily, member 12a*	*Tnfrsf12a*	*9.82*	*0.002*	*0.29*	*0.064*	*2.08*	*0.277*
NM_012591	*interferon regulatory factor 1*	*Irf1*	*9.32*	*0.000*	*0.39*	*0.005*	*1.33*	*0.311*
NM_133306	*oxidized low density lipoprotein (lectin-like) receptor 1*	*Oldlr1*	*9.02*	*0.000*	*0.30*	*0.004*	*2.01*	*0.041*
NM_024127	*growth arrest and DNA-damage-inducible 45 alpha*	*Gadd45a*	*6.25*	*0.001*	*0.50*	*0.098*	*1.95*	*0.130*
NM_053420	*BCL2/adenovirus E1B 19 kDa-interacting protein 3*	*Bnip3*	*6.07*	*0.000*	*0.19*	*0.002*	*0.88*	*0.734*
AI232697	*phosphatidylserine receptor*	*Jmjd6*	*3.51*	*0.007*	*0.43*	*0.058*	*0.89*	*0.802*
NM_021846	*similar to MAP/microtubule affinity-regulating kinase 4 (MAP/microtubule affinity-regulating kinase like 1) (predicted)*	*RGD1561096*	*3.46*	*0.001*	*0.43*	*0.018*	*0.86*	*0.662*
BI287978	*growth arrest and DNA-damage-inducible 45 beta*	*Gadd45b*	*3.20*	*0.002*	*0.54*	*0.061*	*1.33*	*0.383*
NM_021744	*CD14 antigen*	*Cd14*	*3.07*	*0.003*	*0.49*	*0.039*	*0.73*	*0.362*
NM_012637	*protein tyrosine phosphatase, non-receptor type 1*	*Ptpn1*	*3.02*	*0.007*	*0.35*	*0.015*	*0.47*	*0.069*
BI275994	*transglutaminase 2, C polypeptide*	*Tgm2*	*2.98*	*0.000*	*0.45*	*0.004*	*2.99*	*0.000*
NM_013026	*syndecan 1*	*Sdc1*	*2.91*	*0.000*	*0.48*	*0.005*	*2.92*	*0.001*
BI284739	*LPS-induced TN factor*	*Litaf*	*2.70*	*0.000*	*0.50*	*0.005*	*1.23*	*0.289*
J04943	*nucleophosmin 1 /// similar to Nucleophosmin (NPM) (Nucleolar phosphoprotein B23) (Numatrin) (Nucleolar protein NO38)*	*Npm1 /// LOC300303*	*2.67*	*0.001*	*0.50*	*0.010*	*1.42*	*0.152*
AB049572	*sphingosine kinase 1*	*Sphk1*	*2.63*	*0.002*	*0.61*	*0.067*	*0.60*	*0.074*
AI411788	*protein phosphatase 2 (formerly 2A), regulatory subunit A (PR 65), beta isoform*	*Ppp2r1b*	*2.63*	*0.000*	*0.39*	*0.002*	*1.55*	*0.049*
BI289109	*max binding protein (predicted)*	*Mnt*	*2.44*	*0.004*	*0.51*	*0.027*	*1.40*	*0.258*
X57764	*endothelin receptor type B*	*Ednrb*	*2.43*	*0.002*	*0.58*	*0.028*	*1.11*	*0.673*
NM_134432	*angiotensinogen (serpin peptidase inhibitor, clade A, member 8)*	*Agt*	*2.11*	*0.002*	*0.43*	*0.004*	*1.31*	*0.233*
AF136231	*caspase 2*	*Casp2*	*2.04*	*0.009*	*0.38*	*0.004*	*0.86*	*0.592*
BM387008	*caspase 3, apoptosis related cysteine protease*	*Casp3*	*2.00*	*0.001*	*0.54*	*0.004*	*1.46*	*0.037*
D13341	*mitogen activated protein kinase kinase 1*	*Map2k1*	*1.96*	*0.007*	*0.62*	*0.053*	*1.81*	*0.026*
NM_053974	*eukaryotic translation initiation factor 4E*	*Eif4ebp1*	*1.92*	*0.003*	*0.64*	*0.028*	*1.12*	*0.584*
AY066016	*nuclear receptor subfamily 3, group C, member 1*	*Nr3c1*	*1.85*	*0.006*	*0.59*	*0.022*	*1.10*	*0.680*
BF283772	*v-rel reticuloendotheliosis viral oncogene homolog A (avian)*	*Rela*	*1.67*	*0.012*	*0.71*	*0.091*	*1.27*	*0.256*
NM_013091	*tumor necrosis factor receptor superfamily, member 1a*	*Tnfrsf1a*	*1.62*	*0.036*	*0.54*	*0.017*	*2.08*	*0.009*
NM_017040	*protein phosphatase 2 (formerly 2A), catalytic subunit, beta isoform*	*Ppp2cb*	*1.60*	*0.002*	*0.64*	*0.005*	*0.98*	*0.899*
BM386683	*Stanniocalcin 1*	*Stc1*	*1.59*	*0.016*	*0.65*	*0.033*	*0.80*	*0.264*
AI012221	*chloride intracellular channel 1*	*Clic1*	*1.59*	*0.002*	*0.77*	*0.049*	*1.82*	*0.001*
BI282898	*BCL2-associated athanogene 5*	*Bag5*	*1.57*	*0.002*	*0.61*	*0.004*	*0.78*	*0.077*
BI296393	*programmed cell death 6 (predicted)*	*Pdcd6*	*1.49*	*0.002*	*0.70*	*0.007*	*1.23*	*0.083*

AI169001	*autophagy-related 12 (yeast)*	*Atg12*	*1.47*	*0.004*	*0.65*	*0.006*	*0.90*	*0.387*
BI285751	*cullin 3 (predicted)*	*Cul3_predicted*	*1.46*	*0.012*	*0.62*	*0.006*	*0.87*	*0.373*
NM_133307	*protein kinase C, delta*	*Prkcd*	*1.42*	*0.025*	*0.73*	*0.058*	*1.23*	*0.207*
BI289418	*CD38 antigen*	*Cd38*	*1.42*	*0.091*	*0.68*	*0.088*	*1.19*	*0.433*
NM_012696	*kininogen 1 /// K-kininogen /// similar to alpha-1 major acute phase protein prepeptide*	*Kng1*	*1.42*	*0.019*	*0.68*	*0.019*	*1.84*	*0.002*
AA859665	*Nuclear pore associated protein*	*Npap60*	*1.40*	*0.012*	*0.69*	*0.012*	*0.89*	*0.401*
NM_080887	*thioredoxin-like 1*	*Txnl1*	*1.39*	*0.002*	*0.74*	*0.007*	*1.24*	*0.034*
AA848545	*similar to programmed cell death 10*	*Pdcd10*	*1.38*	*0.063*	*0.61*	*0.016*	*1.52*	*0.033*
NM_012839	*cytochrome c, somatic*	*Cycs*	*1.38*	*0.001*	*0.77*	*0.007*	*1.03*	*0.772*
BI282255	*ribosomal protein S5*	*Rps5*	*1.34*	*0.001*	*0.85*	*0.025*	*0.78*	*0.005*
NM_022510	*ribosomal protein L4*	*Rpl4*	*1.33*	*0.031*	*0.73*	*0.025*	*0.75*	*0.044*
AF411318	*metallothionein 1a*	*Mt1a*	*1.29*	*0.058*	*0.62*	*0.006*	*0.90*	*0.456*
NM_013065	*protein phosphatase 1, catalytic subunit, beta isoform*	*Ppp2cb*	*1.26*	*0.051*	*0.75*	*0.028*	*0.98*	*0.865*
BI283681	*eukaryotic translation initiation factor 5A*	*Eif5a*	*1.25*	*0.031*	*0.77*	*0.023*	*1.29*	*0.031*
NM_080888	*BCL2/adenovirus E1B 19 kDa-interacting protein 3-like*	*Bnip3l*	*1.19*	*0.077*	*0.73*	*0.010*	*0.60*	*0.001*
BF281741	*glioma tumor suppressor candidate region gene 2*	*Gltscr2*	*1.18*	*0.067*	*0.84*	*0.068*	*0.93*	*0.461*
BM389310	*DEAD (Asp-Glu-Ala-Asp) box polypeptide 41 (predicted)*	*Ddx41_predicted*	*1.18*	*0.096*	*0.77*	*0.021*	*1.33*	*0.019*
GROUP 1B	**GENES INCREASED IN SBR50 vs. SHAM AND UNCHANGED IN SBR50/IL-6 vs. SBR50**							
NM_012912	activating transcription factor 3	Atf3	92.25	0.000	1.36	0.435	0.45	0.054
NM_031970	heat shock 27kDa protein 1	Hspb1	11.79	0.006	4.12	0.100	0.44	0.360
NM_053565	suppressor of cytokine signaling 3	Socs3	10.14	0.000	0.51	0.118	1.80	0.177
NM_012603	myelocytomatosis viral oncogene homolog (avian)	Myc	9.53	0.000	0.65	0.357	1.08	0.894
BM384926	DnaJ (Hsp40) homolog, subfamily B, member 1 (predicted)	Dnajb1	9.09	0.005	2.79	0.155	0.26	0.081
NM_013154	CCAAT/enhancer binding protein (C/EBP), delta	Cebpd	6.32	0.000	0.60	0.151	1.38	0.387
AF080594	vascular endothelial growth factor A	Vegfa	6.14	0.000	0.60	0.188	1.04	0.923
BG671521	heat shock protein 1, alpha	Hspca	4.72	0.001	1.34	0.465	0.82	0.658
BI284349	myeloid differentiation primary response gene 116	Myd116	4.65	0.004	1.71	0.270	0.98	0.969
AF007789	plasminogen activator, urokinase receptor	Plaur	4.28	0.001	0.62	0.151	1.17	0.662
NM_021836	Jun-B oncogene	Junb	4.12	0.000	1.31	0.303	0.94	0.845
NM_022542	ras homolog gene family, member B	Rhob	4.06	0.001	1.19	0.629	1.05	0.900
NM_012551	early growth response 1	Egr1	3.89	0.001	1.15	0.693	0.92	0.839
NM_058208	suppressor of cytokine signaling 2	Socs2	3.13	0.045	0.45	0.178	1.51	0.499
NM_012699	DnaJ (Hsp40) homolog, subfamily B, member 9	Dnajb9	2.53	0.019	0.55	0.132	0.55	0.147
NM_013085	plasminogen activator, urokinase	Plau	2.23	0.085	0.81	0.690	0.87	0.791
NM_133416	B-cell leukemia/lymphoma 2 related protein A1	Bcl2a1	2.22	0.048	0.81	0.630	2.78	0.028
BM392366	platelet-activating factor acetylhydrolase, isoform 1b, alpha2 subunit	Pafah1b2	2.13	0.007	0.84	0.511	1.26	0.398
AI178012	retinoblastoma 1	Rb1	1.96	0.000	1.14	0.331	1.43	0.018
BI294137	Hexokinase 2	Hk2	1.89	0.006	0.71	0.119	1.00	0.985
AI008680	benzodiazepine receptor, peripheral	Bzrp	1.86	0.003	0.85	0.383	2.82	0.000
NM_017034	proviral integration site 1	Pim1	1.85	0.012	0.88	0.586	1.09	0.736
NM_012904	annexin A1	Anxa5	1.82	0.036	0.97	0.939	0.78	0.404
BE109605	zinc finger protein 162	Zfp162	1.74	0.016	0.75	0.199	0.95	0.837
NM_013151	plasminogen activator, tissue	Plat	1.68	0.008	0.91	0.630	1.14	0.499
AI178772	prothymosin alpha	Ptma	1.67	0.010	0.86	0.424	1.42	0.084
NM_012734	hexokinase 1	Hk1	1.67	0.012	0.73	0.116	0.86	0.459
NM_012523	CD53 antigen	Cd53	1.66	0.013	0.73	0.117	1.14	0.517
AI237389	heat shock 90kDa protein 1, beta	Hspcb	1.64	0.032	1.30	0.258	1.49	0.106
NM_022531	Desmin	Des	1.60	0.032	0.82	0.380	1.53	0.076

BI296385	similar to chemokine (C-X-C motif) ligand 16	Cxcl16	1.59	0.017	0.82	0.312	1.65	0.024
AA945737	chemokine (C-X-C motif) receptor 4	Cxcr4	1.49	0.051	0.88	0.546	1.62	0.037
NM_012715	Adrenomedullin	Adm	1.48	0.057	1.12	0.605	1.76	0.020
J04024	ATPase, Ca++ transporting, cardiac muscle, slow twitch 2	Atp2a2	1.47	0.035	0.99	0.988	1.03	0.900
NM_024359	hypoxia inducible factor 1, alpha subunit	Hif1a	1.47	0.008	0.86	0.299	1.19	0.235
M83297	protein phosphatase 2 (formerly 2A), regulatory subunit B (PR 52), alpha isoform	Ppp2ca	1.37	0.080	0.81	0.275	1.06	0.778
BE116857	apoptotic chromatin condensation inducer 1	Acin1	1.30	0.089	0.92	0.605	1.14	0.421
AI411586	Sequestosome 1	Sqstm1	1.29	0.040	0.94	0.673	1.21	0.153
M25590	seminal vesicle protein 4	Svp4	1.28	0.072	0.92	0.601	0.93	0.625
U69550	phospholipase D1	Pld1	1.26	0.075	0.93	0.585	0.77	0.074
NM_019161	cadherin 22	Cdh22	1.06	0.048	0.97	0.215	0.96	0.207
NM_012641	regenerating islet-derived 1	Reg1	1.02	0.061	1.00	0.825	0.96	0.018
BI288701	*B-cell translocation gene 2, anti-proliferative*	*Btg2*	*25.68*	*0.000*	*0.41*	*0.135*	*1.31*	*0.672*
NM_024388	*nuclear receptor subfamily 4, group A, member 1*	*Nr4a1*	*9.42*	*0.002*	*2.22*	*0.220*	*0.98*	*0.977*
NM_024134	*DNA-damage inducible transcript 3*	*Ddit3*	*7.53*	*0.002*	*1.21*	*0.757*	*3.78*	*0.033*
NM_133578	*dual specificity phosphatase 5*	*Dusp5*	*6.41*	*0.000*	*1.08*	*0.857*	*0.96*	*0.909*
NM_013060	*inhibitor of DNA binding 2*	*Id2*	*5.69*	*0.000*	*0.69*	*0.201*	*1.77*	*0.063*
NM_031628	*nuclear receptor subfamily 4, group A, member 3*	*Nr4a3*	*4.96*	*0.036*	*1.34*	*0.726*	*0.68*	*0.653*
AI010427	*cyclin-dependent kinase inhibitor 1A*	*Cdkn1a*	*2.90*	*0.013*	*0.55*	*0.151*	*1.83*	*0.171*
NM_053847	*mitogen-activated protein kinase kinase kinase 8*	*Map3k8*	*2.89*	*0.008*	*0.59*	*0.170*	*1.52*	*0.289*
NM_057138	*CASP8 and FADD-like apoptosis regulator*	*Cflar*	*2.82*	*0.051*	*0.44*	*0.136*	*1.77*	*0.317*
NM_053319	*dynein light chain LC8-type 1*	*Dynll1*	*2.80*	*0.001*	*1.26*	*0.375*	*1.35*	*0.255*
NM_053819	*tissue inhibitor of metalloproteinase 1*	*Timp1*	*2.66*	*0.002*	*0.82*	*0.488*	*1.96*	*0.030*
NM_134457	*seven in absentia 2*	*Siah2*	*2.47*	*0.005*	*0.83*	*0.527*	*0.87*	*0.662*
NM_012954	*fos-like antigen 2 /// FBJ osteosarcoma oncogene B*	*Fosl2*	*2.42*	*0.008*	*1.02*	*0.974*	*1.49*	*0.223*
NM_012966	*heat shock 10 kDa protein 1 (chaperonin 10)*	*Hspe1*	*2.31*	*0.000*	*1.23*	*0.255*	*0.55*	*0.008*
BG671549	*superoxide dismutase 2, mitochondrial*	*Sod2*	*2.27*	*0.077*	*0.57*	*0.238*	*3.76*	*0.018*
U05989	*PRKC, apoptosis, WT1, regulator*	*Pawr*	*2.06*	*0.003*	*1.35*	*0.165*	*0.99*	*0.976*
NM_053957	*amyloid beta (A4) precursor protein-binding, family B, member 3*	*Apbb3*	*2.03*	*0.014*	*0.69*	*0.184*	*1.24*	*0.463*
NM_017180	*pleckstrin homology-like domain, family A, member 1*	*Phlda1*	*1.96*	*0.051*	*1.09*	*0.844*	*0.98*	*0.968*
AB020967	*tribbles homolog 3 (Drosophila)*	*Trib3*	*1.91*	*0.036*	*0.60*	*0.118*	*1.87*	*0.069*
NM_053394	*Kruppel-like factor 5*	*Klf5*	*1.85*	*0.062*	*0.62*	*0.165*	*0.86*	*0.680*
NM_012953	*fos-like antigen 1*	*Fosl1*	*1.84*	*0.061*	*0.65*	*0.204*	*0.82*	*0.595*
NM_017258	*B-cell translocation gene 1, anti-proliferative*	*Btg1*	*1.70*	*0.010*	*0.73*	*0.117*	*1.17*	*0.450*
NM_022612	*BCL2-like 11 (apoptosis facilitator)*	*Bcl2l11*	*1.55*	*0.020*	*0.75*	*0.129*	*0.83*	*0.353*
AA892271	*BCL2-like 13 (apoptosis facilitator) (predicted)*	*Bcl2l13*	*1.49*	*0.036*	*0.87*	*0.499*	*1.19*	*0.387*
AA957342	*peptidylprolyl isomerase D (cyclophilin D)*	*Ppid*	*1.46*	*0.051*	*1.24*	*0.286*	*1.20*	*0.384*
NM_053289	*pancreatitis-associated protein*	*Pap*	*1.43*	*0.100*	*0.70*	*0.120*	*1.11*	*0.672*
NM_017006	*glucose-6-phosphate dehydrogenase X-linked*	*G6pdx*	*1.41*	*0.005*	*0.89*	*0.293*	*1.83*	*0.000*
NM_012829	*Cholecystokinin*	*Cck*	*1.39*	*0.037*	*0.89*	*0.463*	*0.62*	*0.013*
AF235993	*Bcl2-associated X protein*	*Bax*	*1.37*	*0.072*	*1.17*	*0.399*	*2.76*	*0.000*
NM_019282	*gremlin 1 homolog, cysteine knot superfamily (Xenopus laevis)*	*Grem1*	*1.26*	*0.087*	*0.84*	*0.215*	*0.92*	*0.568*
NM_131911	*acidic nuclear phosphoprotein 32 family, member B*	*Anp32b*	*1.23*	*0.025*	*0.86*	*0.117*	*1.18*	*0.095*
BI280304	*Bcl2-associated athanogene 1 (predicted)*	*Bag1*	*1.20*	*0.086*	*1.01*	*0.955*	*1.34*	*0.019*
BF287444	*glycogen synthase kinase 3 beta*	*Gsk3b*	*1.18*	*0.067*	*0.92*	*0.349*	*1.04*	*0.669*
NM_031038	*Gonadotropin releasing hormone receptor*	*Gnrhr*	*1.15*	*0.050*	*0.89*	*0.113*	*0.97*	*0.736*
AF081196	*RAS guanyl releasing protein 1*	*Rasgrp1*	*1.10*	*0.018*	*0.94*	*0.140*	*0.94*	*0.154*
NM_012650	*sex hormone binding globulin*	*Shbg*	*1.02*	*0.065*	*0.99*	*0.566*	*0.97*	*0.028*

GROUP 2A	GENES DECREASED IN SBR50 vs. SHAM AND INCREASED IN SBR50/IL-6 vs. SBR50							
NM_052980	nuclear receptor subfamily 1, group I, member 2	Nr1i2	0.39	0.000	1.38	0.027	1.39	0.031
NM_021745	nuclear receptor subfamily 1, group H, member 4	Nr1h4	0.40	0.002	2.99	0.003	1.35	0.251
NM_022407	aldehyde dehydrogenase family 1, member A1	Aldh1a1	0.43	0.015	2.13	0.038	0.42	0.024
NM_012805	retinoid X receptor alpha	Rxra	0.49	0.000	1.27	0.084	0.81	0.130
NM_012493	alpha-fetoprotein	Afp	0.50	0.007	2.02	0.012	0.86	0.547
AI235465	steroid sensitive gene 1	Ssg1	0.50	0.012	2.07	0.015	0.53	0.030
NM_133400	apobec-1 complementation factor	Acf	0.55	0.004	1.63	0.019	0.85	0.387
BM392373	CEA-related cell adhesion molecule 1	Ceacam1	0.58	0.003	1.58	0.013	0.69	0.038
BG377107	DnaJ (Hsp40) homolog, subfamily A, member 3	Dnaja3	0.60	0.000	1.44	0.005	0.93	0.482
NM_012931	breast cancer anti-estrogen resistance 1	Bcar1	0.60	0.018	1.65	0.027	1.25	0.310
NM_022614	inhibin beta C	Inhbc	0.61	0.020	1.64	0.028	0.94	0.809
BF282337	integral membrane protein 2B	Itm2b	0.63	0.000	1.27	0.007	1.13	0.117
BI276999	testis enhanced gene transcript	Tegt	0.63	0.000	1.39	0.002	0.79	0.005
AY083159	Stam binding protein	Stambp	0.63	0.009	1.56	0.017	1.43	0.049
BI275921	anterior pharynx defective 1a homolog (C. elegans)	Aph1a	0.64	0.002	1.38	0.021	2.05	0.000
AF347936	interleukin 11 receptor, alpha chain 1	Il11ra1	0.65	0.009	1.60	0.011	1.27	0.154
AW672589	nuclear factor of kappa light chain gene enhancer in B-cells inhibitor, alpha	Nfkbia	0.65	0.003	1.82	0.002	2.10	0.000
BI279735	Ubiquilin 1	Frap1	0.68	0.001	1.41	0.004	1.34	0.008
NM_017181	fumarylacetoacetate hydrolase	Fah	0.69	0.002	1.29	0.022	0.75	0.019
NM_031546	Regucalcin	Rgn	0.69	0.004	1.57	0.004	0.31	0.000
NM_022277	caspase 8	Casp8	0.70	0.013	1.32	0.058	1.92	0.001
AW523747	adhesion molecule with Ig like domain 2	Amigo2	0.72	0.045	1.54	0.019	1.30	0.131
BI274345	ataxin 10	Atxn10	0.73	0.008	1.22	0.079	0.90	0.387
BI295511	forkhead box O1A	Foxo1a	0.73	0.020	1.39	0.022	0.88	0.353
AI009817	succinate dehydrogenase complex, subunit C, integral membrane protein	Sdhc	0.73	0.034	1.37	0.043	1.02	0.925
AI011448	Notch gene homolog 2 (Drosophila)	Notch2	0.74	0.088	1.59	0.019	1.18	0.384
BI285459	Nicastrin	Ncstn	0.76	0.003	1.20	0.037	1.34	0.005
AB015946	tubulin, gamma 1	Tubg1	0.78	0.090	1.79	0.004	1.31	0.104
NM_022399	Calreticulin	Calr	0.80	0.016	1.31	0.012	1.05	0.595
M15481	insulin-like growth factor 1	Igf1	0.83	0.069	1.36	0.014	0.51	0.000
NM_024352	Macrophage stimulating 1 (hepatocyte growth factor-like)	Mst1	0.83	0.038	1.28	0.017	0.84	0.077
NM_053491	Plasminogen	Plat	0.83	0.009	1.13	0.073	0.82	0.014
BI281756	Parkinson disease (autosomal recessive, early onset) 7	Park7	0.85	0.036	1.35	0.004	1.13	0.166
NM_133317	*transducer of ErbB-2.1*	*Tob1*	*0.34*	*0.002*	*2.81*	*0.006*	*1.41*	*0.284*
AF335281	*STEAP family member 3*	*Steap3*	*0.41*	*0.002*	*1.62*	*0.066*	*0.69*	*0.170*
AI412114	*etoposide induced 2.4 Mrna*	*Ei24*	*0.46*	*0.000*	*2.14*	*0.002*	*0.98*	*0.917*
NM_031094	*retinoblastoma-like 2*	*Rbl2*	*0.49*	*0.006*	*1.54*	*0.079*	*1.03*	*0.909*
NM_012870	*tumor necrosis factor receptor superfamily, member 11b (osteoprotegerin)*	*Tnfrsf11b*	*0.50*	*0.004*	*1.99*	*0.007*	*1.23*	*0.360*
NM_053902	*kynureninase (L-kynurenine hydrolase)*	*Kynu*	*0.52*	*0.003*	*1.73*	*0.014*	*0.47*	*0.003*
AI169638	*sphingosine-1-phosphate phosphatase 1*	*Sgpp1*	*0.53*	*0.002*	*1.51*	*0.028*	*1.47*	*0.048*
BM388758	*excision repair cross-complementing rodent repair deficiency, complementation group 3*	*Ercc3*	*0.57*	*0.002*	*1.54*	*0.016*	*1.66*	*0.008*
BF398831	*estrogen receptor-binding fragment-associated gene 9*	*Ebag9*	*0.61*	*0.013*	*1.41*	*0.082*	*0.81*	*0.300*
AB004454	*presenilin 2*	*Psen2*	*0.62*	*0.002*	*1.32*	*0.051*	*1.60*	*0.006*
NM_019158	*aquaporin 8*	*Aqp8*	*0.64*	*0.018*	*1.66*	*0.016*	*0.92*	*0.692*
NM_057146	*complement component 9*	*C9*	*0.64*	*0.002*	*1.29*	*0.042*	*1.36*	*0.022*
AF275151	*androgen receptor-related apoptosis-associated protein CBL27*	*Cbl27*	*0.65*	*0.001*	*1.36*	*0.011*	*1.03*	*0.772*
NM_017319	*protein disulfide isomerase associated 3*	*Pdia3*	*0.66*	*0.001*	*1.67*	*0.002*	*1.22*	*0.062*
NM_053907	*deoxyribonuclease I-like 3*	*Dnase1l3*	*0.66*	*0.005*	*1.36*	*0.034*	*0.66*	*0.012*

AF262320	*programmed cell death 8*	*Pdcd8*	*0.69*	*0.000*	*1.19*	*0.009*	*0.92*	*0.164*
BM391371	*Goliath*	*LOC652955*	*0.71*	*0.001*	*1.26*	*0.016*	*0.82*	*0.034*
AA819870	*complement component 8, beta polypeptide (mapped)*	*C8b*	*0.79*	*0.018*	*1.28*	*0.024*	*0.80*	*0.038*
AI409930	*B-cell receptor-associated protein 31*	*Bcap31*	*0.81*	*0.007*	*1.28*	*0.006*	*1.08*	*0.333*
GROUP 2B	**GENES DECREASED IN SBR50 vs. SHAM AND UNCHANGED IN SBR50/IL-6 vs. SBR50**							
NM_012842	epidermal growth factor	Egfr	0.32	0.000	1.29	0.204	0.59	0.021
BM385790	Kruppel-like factor 2 (lung) (predicted)	Klf2	0.40	0.006	1.10	0.789	1.33	0.384
NM_032612	signal transducer and activator of transcription 1	Stat1	0.45	0.075	2.20	0.101	6.09	0.003
NM_053923	phosphatidylinositol 3-kinase, C2 domain containing, gamma polypeptide	Pic3c2g	0.50	0.014	1.15	0.630	0.30	0.002
NM_031541	scavenger receptor class B, member 1	Scarb1	0.52	0.002	1.29	0.151	0.77	0.152
NM_053523	homocysteine-inducible, endoplasmic reticulum stress-inducible, ubiquitin-like domain member 1	Herpud1	0.53	0.017	1.42	0.186	0.47	0.015
NM_013063	poly (ADP-ribose) polymerase family, member 1	Parp12_predicted	0.56	0.011	0.87	0.539	1.02	0.951
NM_017206	solute carrier family 6 (neurotransmitter transporter, taurine), member 6	Slc6a6	0.56	0.078	0.81	0.539	1.60	0.185
AA799421	protein kinase C, epsilon	Prkce	0.58	0.002	0.79	0.119	1.50	0.019
NM_022185	phosphatidylinositol 3-kinase, regulatory subunit, polypeptide 2	Pik3r2	0.59	0.056	1.18	0.575	1.33	0.348
AI177631	bifunctional apoptosis regulator	bflar	0.59	0.086	0.93	0.857	1.50	0.230
NM_017322	mitogen-activated protein kinase 9	Mapk9	0.60	0.011	1.15	0.468	1.24	0.289
NM_017094	growth hormone receptor	Ghr	0.61	0.072	1.15	0.650	0.60	0.096
AI716502	sphingosine kinase 2	Sphk2	0.64	0.046	1.44	0.119	1.06	0.837
BG378230	mitochondrial ribosomal protein S30 (predicted)	Mrps30	0.64	0.016	1.10	0.611	0.46	0.002
NM_019364	sec1 family domain containing 1	Scfd1	0.65	0.025	1.28	0.189	1.05	0.798
BM385237	annexin A4	Anxa5	0.66	0.087	1.49	0.120	2.32	0.007
BI289543	zinc finger, MYND domain containing 11	Zmynd11	0.67	0.006	1.05	0.744	1.24	0.137
U68544	peptidylprolyl isomerase F (cyclophilin F)	Ppif	0.67	0.003	1.07	0.587	0.88	0.348
NM_031053	mutL homolog 1 (E. coli) /// hypothetical gene supported by NM_031053	Mlh1	0.68	0.045	1.38	0.103	1.30	0.200
X02904	glutathione-S-transferase, pi 1 /// glutathione S-transferase, pi 2	Gstp1	0.71	0.012	1.22	0.136	0.79	0.089
NM_053777	mitogen activated protein kinase 8 interacting protein	Mapk8ip	0.71	0.033	1.29	0.117	0.86	0.387
BE110607	similar to apoptosis related protein APR-3; p18 protein (predicted)	RGD1311605_predicted	0.72	0.072	1.29	0.170	0.69	0.070
NM_012803	protein C	Sftpc	0.72	0.005	1.18	0.123	0.70	0.007
U69109	protein tyrosine kinase 2 beta	Ptk2b	0.74	0.081	1.11	0.561	1.21	0.321
AA819804	Zinc finger protein 91	Zfp91	0.75	0.090	1.16	0.420	1.26	0.216
BG673589	paxillin	Pxn	0.75	0.028	1.16	0.267	1.17	0.258
BF419646	retinoic acid receptor, beta	Rarb	0.75	0.086	1.14	0.468	2.37	0.001
NM_053739	beclin 1 (coiled-coil, myosin-like BCL2-interacting protein)	*Becn1*	0.75	0.037	1.17	0.258	1.11	0.470
AI171615	chromosome segregation 1-like (S. cerevisiae) (predicted)	Cse1l_predicted	0.78	0.062	1.26	0.104	1.45	0.019
NM_053864	valosin-containing protein	Vcpip1	0.78	0.010	1.06	0.501	1.14	0.176
AI170385	SWI/SNF related, matrix associated, actin dependent regulator of chromatin, subfamily a, member 2	Smarca2	0.80	0.089	1.21	0.170	0.99	0.923
NM_012660	eukaryotic translation elongation factor 1 alpha 2	Eef1a2	0.81	0.090	1.02	0.931	0.86	0.276
NM_133409	integrin linked kinase	Ilk	0.83	0.087	1.07	0.582	1.27	0.054
AA800669	protein phosphatase 2 (formerly 2A), regulatory subunit A (PR 65), alpha isoform	Ppp2r1a	0.88	0.091	1.00	0.979	1.23	0.024
NM_013149	*aryl hydrocarbon receptor*	*Ahr*	*0.32*	*0.001*	*1.21*	*0.502*	*0.92*	*0.776*
NM_022180	*hepatocyte nuclear factor 4, alpha*	*Hnf4a*	*0.33*	*0.000*	*1.35*	*0.119*	*1.45*	*0.066*
BI297236	*Transformation related protein 53 inducible nuclear protein 1*	*Trp53inp1*	*0.49*	*0.053*	*1.47*	*0.317*	*1.06*	*0.894*
BE108058	*Procollagen, type XVIII, alpha 1*	*Col18a1*	*0.49*	*0.045*	*1.56*	*0.217*	*0.67*	*0.283*
AB019366	*poly (ADP-ribose) glycohydrolase*	*Parg*	*0.52*	*0.004*	*1.12*	*0.611*	*1.49*	*0.072*
NM_012498	*aldo-keto reductase family 1, member B4 (aldose reductase)*	*Akr1b4*	*0.53*	*0.003*	*1.33*	*0.138*	*1.10*	*0.660*
NM_053307	*methionine sulfoxide reductase A*	*Msra*	*0.60*	*0.002*	*1.26*	*0.125*	*0.47*	*0.001*

BF400782	*protein kinase, DNA activated, catalytic polypeptide (predicted)*	*Prkdc_predicted*	*0.60*	*0.005*	*1.06*	*0.733*	*0.89*	*0.506*
NM_017079	*CD1d1 antigen*	*Cd1d1*	*0.60*	*0.031*	*1.46*	*0.118*	*1.28*	*0.317*
NM_053448	*histone deacetylase 3*	*Hdac3*	*0.61*	*0.028*	*1.39*	*0.147*	*1.24*	*0.367*
AI408078	*BCL2-associated transcription factor 1*	*Bclaf1*	*0.64*	*0.028*	*0.93*	*0.748*	*0.72*	*0.130*
BF283688	*tumor necrosis factor ligand superfamily member 12*	*Tnfsf12*	*0.65*	*0.069*	*1.46*	*0.123*	*1.19*	*0.497*
BI286396	*PERP, TP53 apoptosis effector (predicted)*	*Perp*	*0.69*	*0.042*	*1.13*	*0.540*	*0.51*	*0.005*
BE107162	*high mobility group box 1*	*Hmgb1*	*0.69*	*0.005*	*1.17*	*0.199*	*0.89*	*0.374*
BF408447	*programmed cell death 5 (predicted)*	*Pdcd5*	*0.70*	*0.013*	*1.25*	*0.123*	*1.19*	*0.236*
U06230	*protein S (alpha)*	*Pros1*	*0.70*	*0.019*	*1.14*	*0.405*	*0.70*	*0.034*
AI227743	*Fas-activated serine/threonine kinase*	*Fastk*	*0.72*	*0.017*	*1.00*	*0.989*	*1.11*	*0.459*
AI176519	*immediate early response 3*	*Ier3*	*0.73*	*0.051*	*1.32*	*0.110*	*1.16*	*0.396*
NM_130406	*Fas-associated factor 1*	*Faf1*	*0.74*	*0.061*	*1.16*	*0.389*	*1.51*	*0.030*
BM389034	*TNF receptor-associated protein 1*	*Trap1*	*0.74*	*0.036*	*1.08*	*0.636*	*0.91*	*0.554*
AA800180	*thioredoxin 2*	*Txn2*	*0.75*	*0.029*	*1.10*	*0.465*	*1.18*	*0.230*
D14592	*mitogen activated protein kinase kinase 2*	*Map2k2*	*0.75*	*0.033*	*1.23*	*0.132*	*1.37*	*0.037*
BG665132	*mitochondrial carrier homolog 1 (C. elegans)*	*Mtch1*	*0.77*	*0.022*	*1.08*	*0.537*	*1.17*	*0.207*
BM390196	*thioredoxin domain containing 5 (predicted)*	*Txndc5_predicted*	*0.77*	*0.043*	*1.22*	*0.126*	*0.65*	*0.008*
BF284481	*SH3-domain GRB2-like B1 (endophilin)*	*Sh3glb1*	*0.77*	*0.087*	*0.93*	*0.673*	*1.23*	*0.213*
BM383722	*NCK-associated protein 1*	*Nell1*	*0.80*	*0.070*	*1.06*	*0.646*	*0.95*	*0.719*
NM_031978	*proteasome (prosome, macropain) 26S subunit, non-ATPase, 1*	*Psmd1*	*0.81*	*0.093*	*1.14*	*0.336*	*1.33*	*0.052*
AA946474	*Calpastatin*	*Cast*	*0.82*	*0.089*	*0.96*	*0.781*	*1.15*	*0.288*
GROUP 3	**GENES INCREASED IN SBR50 vs. SHAM AND INCREASED IN SBR50/IL-6 vs. SBR50**							
BI278231	heat shock 70kD protein 1B (mapped)	Hspa1b	51.80	0.002	7.75	0.072	0.06	0.026
NM_031971	heat shock 70kD protein 1A /// heat shock 70kD protein 1B (mapped)	Hspa1a	45.41	0.002	7.32	0.061	0.08	0.026
AI236601	heat shock 105kDa/110kDa protein 1	Hsph1	8.49	0.006	3.36	0.097	0.43	0.264
BI288619	Jun oncogene	Jun	5.64	0.001	2.68	0.021	0.51	0.102
NM_031327	cysteine rich protein 61	Cyr61	3.48	0.003	4.43	0.004	0.52	0.105
AA818262	angiopoietin-like 4	Angptl4	2.98	0.000	1.50	0.028	1.37	0.089
NM_012935	crystallin, alpha B	Cryab	1.82	0.016	1.84	0.021	0.88	0.619
AF077354	heat shock protein 4	Hspa4	1.50	0.037	1.46	0.063	1.20	0.381
AI599423	*growth arrest and DNA-damage-inducible 45 gamma*	*Gadd45g*	*8.66*	*0.000*	*2.50*	*0.005*	*0.80*	*0.411*
AI231792	*Bcl2-associated athanogene 3*	*Bag3*	*3.76*	*0.018*	*3.16*	*0.049*	*0.16*	*0.007*

*Genes listed in regular type are anti-apoptotic, while genes listed in italics are pro-apoptotic.

†FDR: False discovery rate.

Two isoforms of Stat3 are expressed in all cells—α (p92) and β (p83)—both derived from a single gene by alternative mRNA splicing with Stat3α predominating [28]. Stat3α functions as an oncogene [29] in part through inhibiting apoptosis, while Statβ antagonizes the oncogenic function of Stat3α [30]. While mice deficient in both isoforms of Stat3 are embryonic lethal at day 6.5 to 7 [31] and mice deficient in Stat3α die within 24 hr of birth, mice deficient in Stat3β have normal survival and fertility [9]. To further support the hypothesis that Stat3, in particular Stat3α, contributes to resistance to apoptosis within the liver in the setting of HS, we subjected Stat3β homozygous-deficient ($Stat3\beta^{\Delta/\Delta}$) mice and their littermate control wild type mice to a severe HS protocol (target MAP 30 mm Hg for 5 hr) and examined their livers for nucleosome levels 1 hr after the start of resuscitation. As expected, nucleosome levels in wild type HS mice (1027.3 ± 273.3 mU/mg total protein) were increased compared to wild type sham mice (210.3 ± 29.8; $p < 0.01$; **Figure 4B**). In contrast, however, nucleosome levels in the livers of $Stat3\beta^{\Delta/\Delta}$ HS (463.9 ± 3.9) mice were reduced 2.2 times compared to wild type HS mice and were similar to wild type sham mice (**Figure 4B**). These findings indicate that Stat3, in particular Stat3α, protects the liver from apoptosis in the setting of trauma/HS.

Microarray analysis of the liver transcriptome focusing on differential expression of apoptosis-related genes

In addition to increasing the transcription of anti-apoptotic genes (Bcl-xL, Bcl-2, and Mcl-1) [29, 32-39], Stat3 has been shown to decrease transcription of pro-apoptotic genes (Bad, Bnip3l, Casp3). To evaluate the role of Stat3 downstream of IL-6 at the transcriptome level, and to identify genes altered within the livers of animals subjected to trauma/HS especially those involved in apoptosis in a global and unbiased manner, we performed Affymetrix oligonucleotide microarray analysis with RAE 230A chips. Fifteen chips were hybridized using mRNA isolated from 4 livers each from sham, SBR50, and SBR50/IL-6 groups, and 3 livers from SBR50/IL-6/G groups. All fifteen chips were included in the normalization and expression estimation steps of the analysis and were included in the statistical analysis and differential expression comparison. The 15,866 probesets on the RAE 230A chip represent 9,818 annotated genes or expressed sequence tags, including 860 apoptosis-related genes. The list of 860 apoptosis-related genes present on the RAE 230A (**Table 1**) was created by combining gene lists obtained by querying annotation databases provided in GeneSpring and dChip, which were derived from the Gene Ontology (GO) Consortium.

To identify genes differentially expressed among the experimental groups, the data were filtered to remove genes with nearly uniformly low expression (absent on ≥ 80% of chips). Of the 860 apoptosis-related genes represented on the chips, 731 genes met the requirement of this filtering process and were included in the analysis. One-way ANOVA (see Materials and Methods) was then performed which identified 350 apoptosis genes with differential expression among four experimental groups-- sham, SBR50, SBR50/IL-6, and SBR50/IL-6/G-- at a False Discovery Rate (FDR) = 10% (**Table 2**). Of the 350 apoptosis pathway genes whose expression was altered among the four groups, 311 were altered in the SBR50 vs. sham comparison (**Figure 5A** and **Table 2**). Among the genes whose differential expression was altered in the SBR50 vs. sham comparison, the transcripts of the majority of these genes (193 genes) were increased in SBR50 vs. sham by 4.2 ± 1.2 fold (range = 1.02 to 92.3 fold) while transcripts of 118 genes were decreased in SBR50 vs. sham by 1.5 ± 1.2 fold (range = 1.1 to 3.3 fold; **Figure 5B**). Importantly, 106 of the 193 genes (55%) that were increased in the SBR50 vs. sham group, were decreased significantly in the SBR50/IL-6 vs. SBR50 group by 1.8 ± 0.9 fold (range = 1.3 to 14.3 fold) and 108 of the 118 genes (92%) that were decreased in SBR50 group, were increased significantly in the SBR50/IL-6 group by 1.4 ± 0.7 fold (range = 1.2 to 2.9 fold; **Figure 5B**). Thus, of the genes whose transcript levels were altered in SBR50 vs. sham group, 214 of 311 (69%) returned to sham level or were "normalized" in the SBR50/IL-6 group.

One hundred and twenty-five of the 214 genes altered in the SBR50 vs. sham comparison, and normalized in the SBR50/IL-6 vs. SBR50 comparison, were also altered in the SBR50/IL-6 vs. SBR50/IL-6/G comparison. Fifty seven of these 125 genes (46%) were altered in the opposite direction as the SBR50/IL-6 vs. SBR50 comparison, consistent

with the hypothesis that IL-6 normalizes the trauma/HS-induced lung apoptosis transcriptome in part through activation of Stat3.

Apoptosis-related genes consist of those encoding proteins that prevent apoptosis (anti-apoptotic genes) and those encoding proteins that induce apoptosis (pro-apoptotic genes). To identify candidate apoptosis-related genes whose altered expression caused trauma/HS-induced AEC apoptosis, we focused on anti-apoptotic genes whose transcript levels were decreased by trauma/HS and on pro-apoptotic genes whose transcript levels were increased by trauma/HS. Among the genes differentially expressed in the SBR50 vs. sham comparison, 69 anti-apoptotic genes were decreased and 90 pro-apoptotic genes were increased (**Figure 5C**). Expression levels of 65 out of 69 (94%) anti-apoptotic genes decreased by trauma/HS were increased by IL-6 treatment; 76 of 90 (84%) of the pro-apoptotic genes that were increased by trauma/HS, were decreased by IL-6 treatment. Finally, the expression of 46% of anti-apoptotic genes increased by IL-6 treatment were decreased by pre-treatment with T40214; conversely 63% of pro-apoptotic genes decreased by IL-6 treatment were increased by T40214 pre-treatment (**Figure 5C**).

Pro-apoptotic genes whose expression was increased ≥ 6-fold by trauma/HS (≥2.5-fold upregulated) were *EGL nine homolog 3* (*Egln3*; 17.3-fold), *dual specificity phosphatase 6* (*Dusp6*; 15.5-fold), *tumor necrosis factor receptor superfamily 12a* (*Tnfrsf12a*; 9.8-fold), *interferon regulatory factor 1* (*Irf1*; 9.3-fold), *oxidized low density lipoprotein receptor 1* (*Oldlr1*; 9.0-fold), *growth arrest and DNA-damage-inducible 45 alpha* (*Gadd45a*; 6.3-fold), and *BCL2 adenovirus E1B interacting protein 3* (*Bnip3*; 6.1-fold, **Table 2**). The expression of each was decreased in the IL-6-treated group by 1.7-14.3 fold (**Table 2**).

Discussion

In these studies, we demonstrated that trauma/HS-induced liver apoptosis occurs within 1 hr of resuscitation from trauma/HS and depends on the severity of shock with the degree of apoptosis increasing exponentially with increased duration of shock. There was an absolute requirement for resuscitation in order for apoptosis to occur; the finding that no apoptosis occurred in the absence of resuscitation suggested that complete prevention could be achieved by an appropriate intervention introduced at the start of resuscitation. IL-6 administration at the start of resuscitation completely prevented trauma/HS-induced liver apoptosis and was accompanied by increased levels of Stat3 activity within the liver. Pharmacological inhibition of Stat3 using the G-quartet oligodeoxynucleotide (GQ-ODN) T40214 markedly attenuated IL-6-mediated Stat3 activation and prevention of liver apoptosis. Mice deficient in Stat3β, an endogenous naturally occurring, dominant negative isoform of Stat3, were protected from trauma/HS-induced liver apoptosis confirming a role for Stat3, especially Stat3α, in protection against trauma/HS-induced liver apoptosis. Liver microarray analysis showed that 48% of known apoptosis–related genes were altered in trauma/HS. IL-6 "normalized" the expression of 69% of these genes; Stat3 was responsible for this normalization in 46% of the cases. Further examination of the microarray results indicated that the effect of IL-6 in the apoptosis transcriptome was two-fold; IL-6 increased levels of 96% of the anti-apoptotic gene transcripts whose levels were decreased by trauma/HS and also decreased transcript levels of 84% of the pro-apoptotic genes whose levels were increased by trauma/HS.

The liver is susceptible to injury following insults such as hemorrhagic shock. Since it is responsible for maintaining energy homeostasis, hepatic injury and dysfunction associated with hemorrhagic shock can affect other organs and lead to multiple organ failure and death [40-42]. We have previously demonstrated in mice that trauma/HS induces liver apoptosis detected 24 hrs after the resuscitation [6]. In the current study, using our rat model of trauma/HS we found that liver apoptosis occur as early as 1 hour after reperfusion, and for the first time, that its severity depends on the duration of hypotension and requires resuscitation. Liver apoptosis due to ischemia/reperfusion injury has been shown to occur in humans and in experimental models of liver transplantation [43], as well as during hemorrhagic shock [41, 42]. In these studies, release of ROS during reperfusion was implicated in the pathogenesis of liver apoptosis during reperfusion in models of liver transplantation

[42, 43], and may be contributing to liver apoptosis in our model.

Interventions aiming at preventing liver apoptosis have been shown to prevent parenchymal injury and improve animal survival in ischemic injury during liver transplant [43]. We previously demonstrated that exogenous administration of IL-6 decreased liver apoptosis in mice following trauma/HS [6], however, the mechanism for the anti-apoptotic effects of IL-6 was not determined. Kovalovich et al. provided evidence that IL-6 protects hepatocytes from carbon tetrachloride-induced apoptosis [44] as well as from Fas-mediated apoptosis [45] through prevention of rapid degradation of the anti-apoptotic proteins Bcl-2, Bcl-xL and FLIP in the livers. While this may contribute to the anti-apoptotic effect of IL-6 administration in our rat trauma/HS model, our finding that the IL-6 preventive effect was blocked by a specific Stat3 inhibitor, T40214, and could be replicated in mice by genetic deletion of Stat3β, a naturally occurring, dominant-negative isoform of Stat3, indicates that a large portion of the effect of IL-6 in our trauma/HS model is being mediated by Stat3 which acts at the transcriptional and not the post-translational level.

IL-6-mediated activation of Stat3 has been shown to protect against toxin-mediated hepatocyte apoptosis through mechanisms that involve increased levels of anti-apoptotic proteins such as Bcl-xL and Bcl-2 in the liver [46, 47]. Stat3 activation mediates increased transcription of anti-apoptotic genes like Bcl-xL, Bcl-2, and Mcl-1, as well as decreased transcription of pro-apoptotic genes, including Bad, Bnip3 and Casp3 [29, 32-39]. Microarray analysis of the liver apoptosis transcriptome revealed that the expression levels of the pro-apoptotic genes Bnip3 and Casp3 were increased by 6- and 2-fold, respectively, following trauma/HS and were decreased by 5.4- and 4.1-fold respectively after IL-6 treatment. However, only the expression of Casp3 was increased by Stat3 pharmacological inhibition with T40214. None of the other apoptosis-related genes known to be modulated by Stat3 to promote apoptosis protection in other settings of liver injury were affected by IL-6 treatment or by pre-treatment with T40214, suggesting that other apoptosis-related genes are involved in the anti-apoptotic effects of IL-6-mediated Stat3 activation in our model of trauma/HS.

A complete assessment of the liver apoptosis transcriptome using oligonucleotide microarray analysis determined that trauma/HS altered the expression of 48% of apoptosis-related genes, of which 56% were anti-apoptotic and 44% were pro-apoptotic genes (**Figure 5B**). The overall effect of trauma/HS in the liver apoptosis transcriptome was to increase the expression of apoptosis-related genes. IL-6 administration induced the opposite effect by decreasing the expression of apoptosis-related genes whose expression was increased by trauma/HS, and by increasing the expression of apoptosis-related genes whose expression was decreased by trauma/HS (**Figure 5C**), suggesting a "normalizing" effect of IL-6 in the trauma/HS-induced liver apoptosis transcriptome. Stat3 inhibition, by GQ-ODN administration, reversed the IL-6 "normalizing" effect on gene expression in 46% of the apoptosis-related genes (**Figure 5C**). These results suggest that IL-6 administration promotes protection from trauma/HS-induced liver apoptosis by opposing the effects of trauma/HS in the liver apoptosis transcriptome in part by Stat3 activation. Anti- and pro-apoptotic subsets of genes were analyzed separately to determine the effect of trauma/HS in each subset of transcripts. Gene transcript levels in both, anti- and pro-apoptotic subsets were increased by trauma/HS. Interestingly, IL-6 normalized the expression of genes in both subsets of genes, an effect that was reversed by pre-treatment with Stat3 inhibitor (**Figure 5C**).

In our model of trauma/HS, pro-apoptotic genes upregulated by trauma/HS are likely to be mediators of trauma/HS-induced liver apoptosis, which is likely prevented by the IL-6 normalizing effect on their expression through Stat3 activation. Among the transcripts most up-regulated following trauma/HS and downregulated in the IL-6 treatment group were Egln3, Dusp6, Tnfrsf12, Irf1, Oldlr1, Gadd45a, and Bnip3. Egln3 is a prolyl hydroxylase which is induced in sympathetic neurons after nerve growth factor withdrawal, and induces apoptosis when overexpressed in pheochromocytoma cells [48]. Dusp6 is a cytosolic phosphatase with pancreatic tumor suppressive properties and mediates apoptosis and cell growth arrest by specifically

inactivating extracellular signalregulated kinase (ERK) [49]. Tnfrs12 is known to sensitize melanoma cells to chemotherapy-induced apoptosis [50]. Irf1 is activated by serum from human patients with sepsis, and mediates apoptosis in fetal myocytes [51]. Oldlr1 is expressed in highly vascularized organs such as the lung and placenta, and in endothelial cells, smooth muscle cells, cardiomyocytes and activated macrophages. Oldlr1 is a type II glycoprotein and acts as a receptor for oxidized low-density lipoprotein (ox-LDL). Interaction with ox- LDL induces ROS, reduces NO and activates NFκB. It also increases expression of Bax and decreases expression of Bcl-2. Oldlr1 is known to induce apoptosis of vascular endothelial cells and vascular smooth muscle cells in a model of cardiac ischemia reperfusion [52]. Gadd45g belongs to a family of proteins involved in DNA damage response and cell growth arrest. It is ubiquitously expressed in all normal adult and fetal tissues. Gadd45g activates MTK1 kinase activity in response to environmental stresses leading to apoptosis through the p38/c-Jun kinase pathway. Downregulation of Gadd45g prevents apoptosis of cancer cells [53].

The protective effects of IL-6 in trauma/HS-induced liver injury were mediated in large measure by Stat3 through its ability to normalize the apoptosis transcriptome. Our findings provide evidence that support the use of IL-6 as a potential therapeutic agent to protect against liver injury and dysfunction by blocking apoptosis early after reperfusion. Such an intervention has the potential to prevent multiple organ failure and improve survival in the setting of severe hemorrhagic shock.

Acknowledgements

This work was supported, in part, by grant HL07619 (DJT) and T32-HL66991 (AM) from the National Heart, Lung and Blood Institute of the National Institutes of Health and H48839 (AM) from the American Lung Association.

Address correspondence to: David J. Tweardy, MD, Departments of Medicine and Molecular and Cellular Biology, Baylor College of Medicine, BCM 286, Room N-1319, One Baylor Plaza, Houston, Texas 77030, FAX: (713) 798-8948, E-MAIL: dtweardy@bcm.edu

References

[1] Minino AM AR, Fingerhut LA, Boudreault MA, Warner M. Deaths: Injuries 2002. National Vital Statistics Reports. Vol. 54, 2006:1-125.

[2] Moore FA, Sauaia A, Moore EE, Haenel JB, Burch JM and Lezotte DC. Postinjury multiple organ failure: a bimodal phenomenon. J Trauma 1996;40:501-10; discussion 510-512.

[3] Ciesla DJ ME, Johnson JL, Burch JM, Cothren CC, and Sauaia A. The role of the lung in postinjury multiple organ failure. Surgery 2005;138:749-758.

[4] Jarrar D, Wang P, Cioffi WG, Bland KI and Chaudry IH. Critical role of oxygen radicals in the initiation of hepatic depression after trauma hemorrhage. J Trauma 2000;49:879-885.

[5] Heckbert SR, Vedder NB, Hoffman W, et al. Outcome after hemorrhagic shock in trauma patients. J Trauma 1998;45:545-549.

[6] Arikan AA YB, Mastrangelo MA, Tweardy DJ. Interleukin-6 treatment reverses apoptosis and blunts susceptibility to intraperitoneal bacterial challenge following hemorrhagic shock. Crit Care Med 2006;34:771-777.

[7] Meng ZH, Dyer K, Billiar TR and Tweardy DJ. Essential role for IL-6 in postresuscitation inflammation in hemorrhagic shock. Am J Physiol Cell Physiol 2001;280:C343-351.

[8] Hierholzer C, Harbrecht B, Menezes JM, et al. Essential role of induced nitric oxide in the initiation of the inflammatory response after hemorrhagic shock. J Exp Med 1998;187:917-928.

[9] Maritano D, Sugrue ML, Tininini S, et al. The STAT3 isoforms alpha and beta have unique and specific functions. Nat Immunol 2004;5:401-409.

[10] Hierholzer C HB, Menezes JM, Kane J, MacMicking J, Nathan CF, Peitzman AB, Billiar TR, Tweardy DJ. Essential role of induced nitric oxide in the initiation of the inflammatory response after hemorrhagic shock. J Exp Med 1998;187:917-928.

[11] Ono M YB, Hardison EG, Mastrangelo MA, Tweardy DJ. Increased susceptibility to liver injury after hemorrhagic shock in rats chronically fed ethanol: role of nuclear factor kappa-B, interlekin-6, and granulocyte colony-stimulating factor. Shock 2004;21:519-525.

[12] Ono M, Yu B, Hardison EG, Mastrangelo MA and Tweardy DJ. Increased susceptibility to liver injury after hemorrhagic shock in rats chronically fed ethanol: role of nuclear factor-kappa B, interleukin-6, and granulocyte colony-stimulating factor. Shock 2004;21:519-525.

[13] Jing N, Li Y, Xiong W, Sha W, Jing L and Tweardy DJ. G-quartet oligonucleotides: a new class of signal transducer and activator of transcription 3 inhibitors that suppresses growth of prostate and breast tumors through induction of apoptosis. Cancer Res 2004;64:6603-6609.

[14] Jing N, Tweardy DJ. Targeting Stat3 in cancer therapy. Anticancer Drugs 2005;16:601-607.
[15] SE SPaA. Mitochondria-associated apoptotic signalling in denervated rat skeletal muscle. J Physiol 2005;565:309-323.
[16] Wu JY, Feng L, Park HT, et al. The neuronal repellent Slit inhibits leukocyte chemotaxis induced by chemotactic factors. Nature 2001;410:948-952.
[17] Wang W, Goswami S, Lapidus K, et al. Identification and testing of a gene expression signature of invasive carcinoma cells within primary mammary tumors. Cancer Res 2004;64:8585-8594.
[18] Benjamini Y, Drai D, Elmer G, Kafkafi N and Golani I. Controlling the false discovery rate in behavior genetics research. Behav Brain Res 2001;125:279-284.
[19] Ishihara K, Hirano T. Molecular basis of the cell specificity of cytokine action. Biochim Biophys Acta 2002;1592:281-296.
[20] Shirogane T, Fukada T, Muller JM, Shima DT, Hibi M and Hirano T. Synergistic roles for Pim-1 and c-Myc in STAT3-mediated cell cycle progression and antiapoptosis. Immunity 1999;11:709-719.
[21] Brazil DP, Park J and Hemmings BA. PKB binding proteins. Getting in on the Akt. Cell 2002;111:293-303.
[22] Brunet A, Bonni A, Zigmond MJ, et al. Akt promotes cell survival by phosphorylating and inhibiting a Forkhead transcription factor. Cell 1999;96:857-868.
[23] Kops GJ, de Ruiter ND, De Vries-Smits AM, Powell DR, Bos JL and Burgering BM. Direct control of the Forkhead transcription factor AFX by protein kinase B. Nature 1999;398:630-634.
[24] Wang XJ, Liefer KM, Tsai S, O'Malley BW and Roop DR. Development of geneswitch transgenic mice that inducibly express transforming growth factor beta1 in the epidermis. Proc Natl Acad Sci U S A 1999;96:8483-8488.
[25] Nicholson KM, Anderson NG. The protein kinase B/Akt signalling pathway in human malignancy. Cell Signal 2002;14:381-395.
[26] Jing N, Li Y, Xu X, et al. Targeting Stat3 with G-quartet oligodeoxynucleotides in human cancer cells. DNA Cell Biol 2003;22:685-696.
[27] Jing N, Sha W, Li Y, Xiong W and Tweardy DJ. Rational drug design of G-quartet DNA as anti-cancer agents. Curr Pharm Des 2005;11:2841-2854.
[28] Huang Y, Qiu J, Dong S, et al. Stat3 isoforms, alpha and beta, demonstrate distinct intracellular dynamics with prolonged nuclear retention of Stat3beta mapping to its unique C-terminal end. J Biol Chem 2007;282:34958-67
[29] Bromberg JF WM, Devgan G, Zhao Y, Pestell RG, Albanese C, Darnell JE. Stat3 as an oncogene. Cell 1999;98:295-303.
[30] Turkson J, Bowman T, Garcia R, Caldenhoven R, DeGroot RP and Jove R. Stat3 activation by Src induces specific gene regulation and is required for cell transformation. Molecular and Cellular Biology 1998 May;18:2545-2552.
[31] Takeda K, Kishimoto T and Akira S. Signal transducer and activator of transcription protein (STAT): its relation to Th1/Th2-mediated diseases [editorial]. Nutrition 1997;13:987-8.
[32] Chen CL HF, Lin J. Systemic evaluation of total Stat3 and Stat3 tyrosine phosphorylation in normal human tissues. Exp Mol Pathol 2006;80:295-305.
[33] Levy DaLC. What does Stat3 do? J Clin Invest 2002;109:1143-1148.
[34] Real P SA, DeJuan A, Segovia J, Lopez-Vega J, Fernandez-Luna J. Resistance to chemotherapy via Stat3-dependent overexpression of Bcl-2 in metastatic breast cancer cells. Oncogene 2002;21:7611-7618.
[35] Leslie K LC, Devgan G, Azare J, Berishaj M, Gerald W, Kim YB, Paz K, et al. Cyclin D1 is transcriptionally regulated by and required for transformation by activated signal transducer and activator of transcription 3. Cancer Res 2006;66:2544-2552.
[36] Catlett-Falcone R, Landowski TH, Oshiro MM, et al. Constitutive activation of Stat3 signaling confers resistance to apoptosis in human U266 myeloma cells. Immunity 1999;10:105-115.
[37] Gritsko T WA, Tucson J, Kaneko S, et al. Persistent activation of Stat3 induces survivin gene expression and confers resistance to apoptosis in human breast cancer cells. Clin Cancer Res 2006;12:11-19.
[38] Fukada T OT, Yoshida Y, Shirogane T, Nishida K, Nakajima K, Hibi M and Hirano T. Stat3 orchestrates contradictory signals in cytokine induced G1 to S cell cycle transition. The EMBO J 1996;17:6670-6677.
[39] Taub R. Hepatoprotection via the IL-6/Stat3 pathway. J Clin Invest 2003;112:978-980.
[40] Kobelt F, Schreck U and Henrich HA. Involvement of liver in the decompensation of hemorrhagic shock. Shock 1994;2:281-288.
[41] Sundar SV, Li YY, Rollwagen FM and Maheshwari RK. Hemorrhagic shock induces differential gene expression and apoptosis in mouse liver. Biochem Biophys Res Commun 2005;332:688-96.
[42] Ayuste EC, Chen H, Koustova E, et al. Hepatic and pulmonary apoptosis after hemorrhagic shock in swine can be reduced through modifications of conventional Ringer's solution. J Trauma 2006;60:52-63.
[43] Rudiger HA GR, Claiven PA. Liver ischemia: apoptosis as a central mechanism of injury. J Invest Surg. 2003;16:149-159.
[44] Kovalovich K, DeAngelis RA, Li W, Furth EE, Ciliberto G and Taub R. Increased toxin-induced liver injury and fibrosis in interleukin-6-deficient mice. Hepatology. 2000;31:149-159.

[45] Kovalovich K, Li W, DeAngelis R, Greenbaum LE, Ciliberto G and Taub R. Interleukin-6 protects against Fas-mediated death by establishing a critical level of antiapoptotic hepatic proteins FLIP, Bcl-2, and Bcl-xL. J Biol Chem 2001;276:26605-26613.
[46] Hong F, Jaruga B, Kim WH, et al. Opposing roles of STAT1 and STAT3 in T cellmediated hepatitis: regulation by SOCS. J Clin Invest 2002;110:1503-1513.
[47] Hong F, Kim WH, Tian Z, et al. Elevated interleukin-6 during ethanol consumption acts as a potential endogenous protective cytokine against ethanol-induced apoptosis in the liver: involvement of induction of Bcl-2 and Bcl-x(L) proteins. Oncogene 2002;21:32-43.
[48] Lee CK, Raz R, Gimeno R, et al. STAT3 is a negative regulator of granulopoiesis but is not required for G-CSF-dependent differentiation. Immunity 2002;17:63-72.
[49] Furukawa Y, Kawasoe T, Daigo Y, et al. Isolation of a novel human gene, ARHGAP9, encoding a rho-GTPase activating protein. Biochem Biophys Res Commun 2001;284:643-649.
[50] Kokkinakis DM. Methionine-stress: a pleiotropic approach in enhancing the efficacy of chemotherapy. Cancer Lett 2006;233:195-207.
[51] Kumar A, Kumar A, Michael P, et al. Human serum from patients with septic shock activates transcription factors STAT1, IRF1, and NF-kappaB and induces apoptosis in human cardiac myocytes. J Biol Chem 2005;280:42619-42626.
[52] Kataoka K, Hasegawa K, Sawamura T, et al. LOX-1 pathway affects the extent of myocardial ischemia-reperfusion injury. Biochem Biophys Res Commun 2003;300:656-660.
[53] Zerbini LF, Libermann TA. Life and death in cancer. GADD45 alpha and gamma are critical regulators of NF-kappaB mediated escape from programmed cell death. CellCycle 2005;4:18-20.
[54] Chakraborty A, Tweardy DJ. Stat3 and G-CS induced myeloid differentiation. Leukemia and Lymphoma 1998;30:433-442.
[55] Chakraborty A, White SM, Schaefer TS, Ball ED, Dyer KF and Tweardy DJ. Granulocyte colony-stimulating factor activation of Stat3 alpha and Stat3 beta in immature normal and leukemic human myeloid cells. Blood 1996;88:2442-2449.